CHAPTER IV

EXPERIMENTAL

4.1 Experimental setup

Figure 4.1 shows the actual arrangement of the experimental apparatus of the gaseous pollutant remover used in the present work. Figure 4.2 presents its schematic diagram.
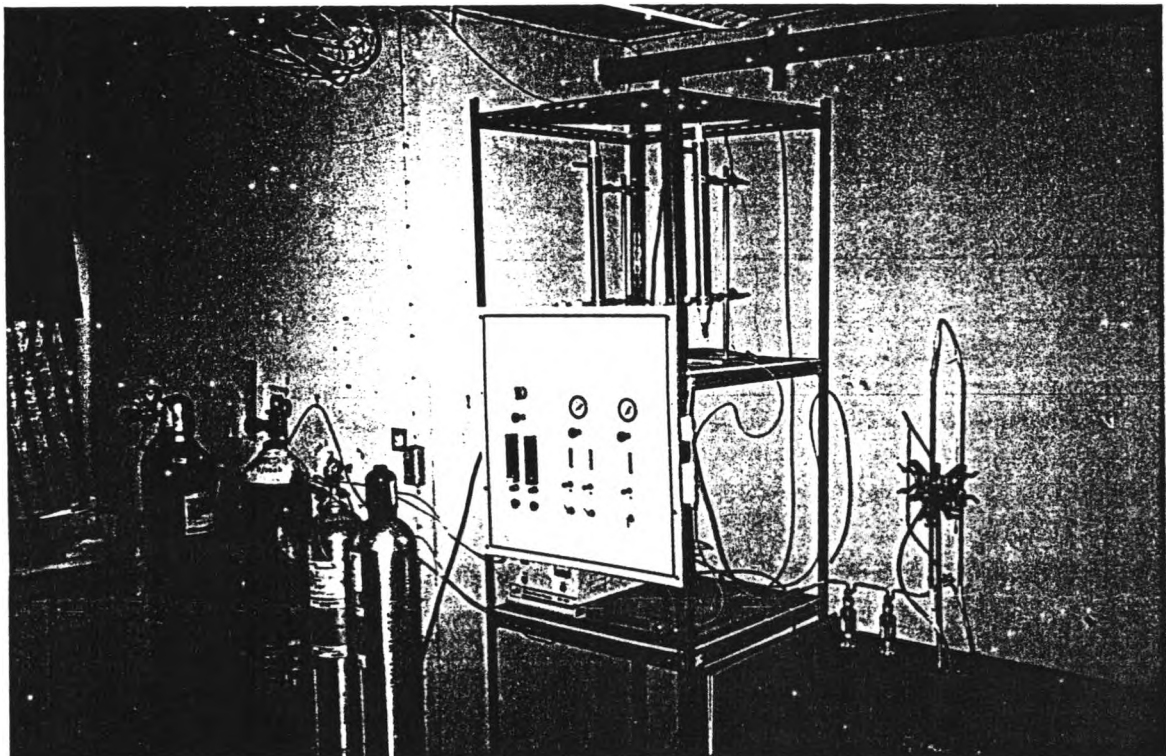

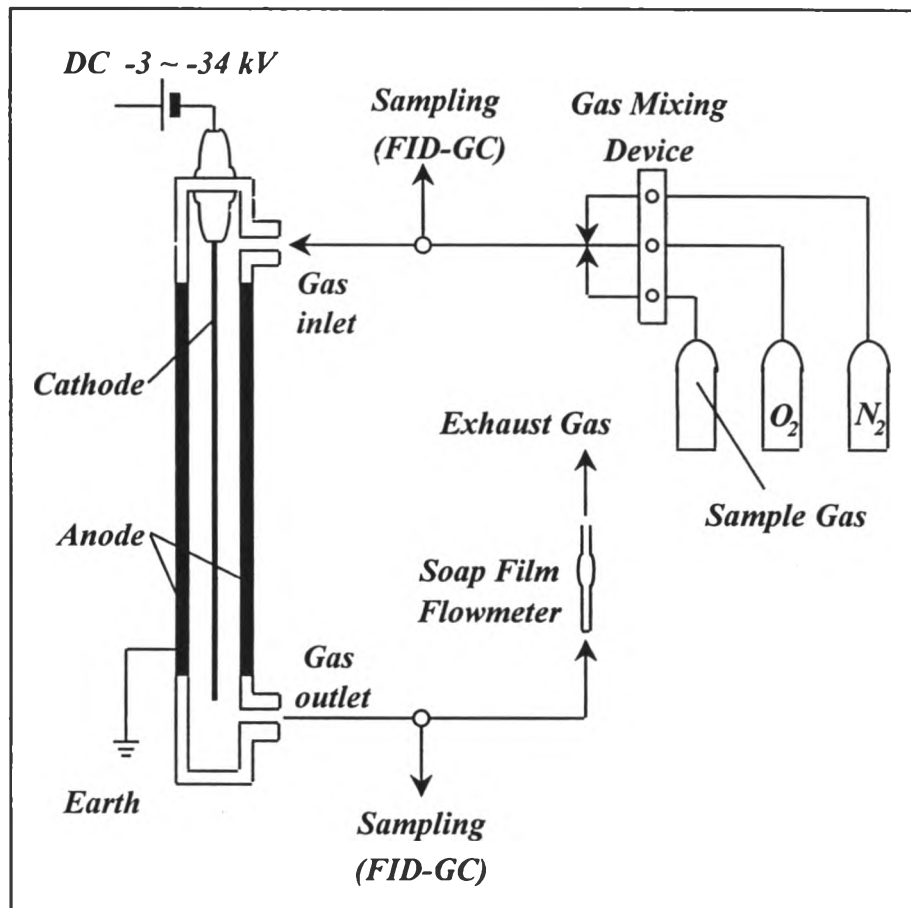Figure 4.1   Arrangement of present experimental apparatus

DC -3 ~ -34 kV

Sampling
(FID-GC)

Gas Mixing
Device

Gas
inlet

Cathode

Anode

Exhaust Gas

O_2

N_2

Sample Gas

Soap Film
Flowmeter

Gas
outlet

Earth

Sampling
(FID-GC)

Figure 4.2 Schematic diagram of experimental apparatus

4.1.1 Details of device

As shown in **Figures 4.1** and **4.2**, the gaseous pollutant remover consists of a deposition-type corona-discharge reactor, a gas mixing device, a high-voltage DC generator and a set of soap film flow meter.

The constructed deposition-type corona-discharge reactor consists of two electrodes, a stainless-wire cathode and a stainless-tube anode (reactor). Up to two reactors are used in the experiments to remove several kinds of malodorous gas components. The dimensions of the two reactors are shown in **Table 4.1**.

Table 4.1 Details of reactors

	Reactor A	Reactor B
Anode		
Material	Brass	Brass
Inner diameter of anode	38 mm	40 mm
Length of anode	280 mm	370 mm
Cathode		
Diameter of wire cathode	0.5 mm	0.5 mm

The reactor cathode is connected to a high-voltage DC generator (Matsusada, HAR-30N5). The high-voltage DC generator whose maximum allowable voltage is 50 kV is utilized to supply a stream of energetic electrons to the corona-discharge reactor. Typically a voltage of -3 kV ~ -34 kV is required to generate discharge current of 0.01 mA ~ 2 mA.

A gas-mixing device is used to adjust and control the concentrations of the gas impurities to be removed. Before feeding a gas mixture to the reactor, the inlet concentrations of individual gases are adjusted by mixing each lab-grade

inlet concentrations of individual gases are adjusted by mixing each lab-grade standard gas with N_2 and/or O_2, depending upon the aim of the removal study. When mixed with N_2, removal from N_2 gas is obtained. When mixed with N_2 and O_2, removal of individual gas from air is achieved. To study the influence of water vapor (H_2O) on the removal efficiency, the concentration of H_2O is controlled by bubbling nitrogen through water in a temperature-controlled bath.

A set of soap film flow meter is used to measure the total flow rate of gas mixture passing through the reactor.

4.1.2 Analytical instruments

In the present study, the concentrations of individual gases at the inlet and outlet of the reactor are analyzed by using a gas chromatograph (Shimadzu Corp., GC 14A and 14B) with a flame ionization detector (FID).

The packed material in the GC column used for detecting the concentrations of all kinds of gases is polyvinylbenzene (Millopore Corp., Porapak Q) with 80~100 mesh size and usable at maximum temperature of $250^\circ C$.

A calibration graph between the FID area of the GC and the concentration of gas impurities is constructed. The concentration of H_2O is measured by a dew point hygrometer (Yokogawa Electric Corporation, MODEL 2586). When reaction by-products are detected by the gas chromatography, a gas chromatography mass spectrometer (GCMS) (Shimadzu Corporation, MS-QP1000S) is used to identify the reaction by-products.

A Derivative Spectrophotometer (Yanaco New Science Inc., UO-1) is used to detect the individual concentration of SO_2, NO_2 and NH_3. **Table 4.2** shows the wavelength, which is used to measure the highest concentration peak.

Table 4.2 Analytical condition for the Derivative Spectrophotometer

Sample gases	Wave length (nm)	Light
SO_2	210	UV
NO_2	450	VIS
NH_3	206	UV

4.2 Experimental procedure and conditions gas

It is important to survey what kind of malodorous gas components can be removed by the electron attachment method. A list of experimental gases and experimental conditions of each gases is shown in **Table 4.3**

Table 4.3 Experimental conditions of malodorous gas components

Sample gas		Concentration	Total flow rate	Space velocity
Name	Formula	[ppm]	$[m^3 s^{-1}]$	$[hr^{-1}]$
Ammonia	NH_3	140	6.67×10^{-6}	75.6
Acetaldehyde	CH_3CHO	20	6.67×10^{-6}	75.6
Trimethylamine	$(CH_3)_3N$	40	6.67×10^{-6}	75.6

The material packed in the GC column used for detecting the concentrations of each gas is polydivinylbenzene (Millopore Corp., Porapak Q) with 80~100 mesh. The measuring conditions of the GC for detecting each malodorous gas component with a flame ionization detector (FID) are summarized in **Table 4.4**

Table 4.4 Measuring conditions of malodorous gas components for FID

gas chromatograph

Sample gas	Column temperature (°C)	Injection temperature (°C)	Detector temperature (°C)	Retention time (min)
CH_3CHO	120	150	150	1.8
$(CH_3)_3N$	120	150	150	4.9

4.2.1 Operating procedure

To operate the gaseous pollutant remover, the following implementation must be made carefully because of the great risk of accident due to the high voltage supplied to the reactor.

- Ensure that the reactor is grounded and each unit of the apparatus is securely connected.
- Adjust the flow rates of individual gases with the gas mixing device and measure their flow rates with the soap film flow meter.
- Feed the gas mixture to the inlet of the reactor and wait till its concentration becomes stable.
- Turn on the high-voltage DC generator and adjust the discharge current as desired, and then keep it stable.
- Take samples at the inlet and outlet of the reactor to be analyzed with the gas chromatograph or derivative spectrophotometer.

- Stop feeding the gas mixture and turn off the DC generator after the completion of the experiment. Be careful that high voltage still remains in the reactor cathode.

4.2.2 Materials and methods

Figure 4.2 shows a schematic diagram of the gaseous pollutant remover. The gas component of interest was mixed with N_2, N_2-O_2 or N_2-H_2O in the gas mixing device and was then fed to the corona-discharge reactor. Some coexisting gases such as oxygen, water vapor, sulfur dioxide, nitrogen dioxide and carbon dioxide were mixed in order to examine its influence on the removal efficiency of each gas type. Acetaldehyde (CH_3CHO), ammonia (NH_3) and trimethylamine $(CH_3)_3N$ were investigated as the malodorous gas components. A gas absorber, ethyl alcohol, was used to trap the residual impurities and possible by-products at the outlet of the reactor. The flow rate of the gas mixture was measured by the soap film flow meter.

The inlet concentrations of the gas samples were adjusted by mixing lab-grade gases with N_2. The concentrations of CH_3CHO and $(CH_3)_3N$ at both the inlet and outlet of the reactor were determined by a gas chromatograph with a flame ionization detector (FID). The Derivative Spectrophotometer (Yanaco New Science Inc., UOI) was used to detect concentration of SO_2, NO_2, and NH_3. The inlet concentration of water vapor was controlled by bubbling the inert gas (N_2) through distilled water in a temperature-controlled bath. The concentration of water vapor was analyzed by a dew point hygrometer. The inlet concentrations of the malodorous gas samples, oxygen, water vapor, sulfur dioxide, nitrogen dioxide and carbon dioxide ranged between 10-140 ppm, 0~20%, 0~6418 ppm, 0~446 ppm, 0-747 ppm and 0~8 %, respectively.

4.3 Experimental results

What follows is a summary of the experimental results of individual removal for a variety of gases, including several components found in crematory emission. More specifically, the influences of several important factors, namely, discharge current, applied voltage, gas flow rate, inlet gas concentration, and common coexisting gases (i.e., oxygen and water vapor) on the removal efficiency of the individual targeted gases are examined experimentally.

4.3.1 Removal efficiency

The definition of removal efficiency, Ψ, used in this work is as follows.

$$\Psi = (C_{in} - C_{out}) / C_{in} \qquad (4.1)$$

where C_{in} and C_{out} are, respectively, the inlet and outlet concentrations of the pollutant in the gas sample.

4.3.2 Removal of trimethylamine

4.3.2.1 Removal of trimethylamine from N_2

Figure 4.3 shows the removal efficiency of trimethylamine $[(CH_3)_3N]$ from N_2. The abscissa is the discharge current, I, and the ordinate is the removal efficiency, Ψ, defined by **Equation 4.1**. From the figure, it can be seen that the concentration of $(CH_3)_3N$ decreases with the discharge current. However, it seems difficult to achieve perfect removal.
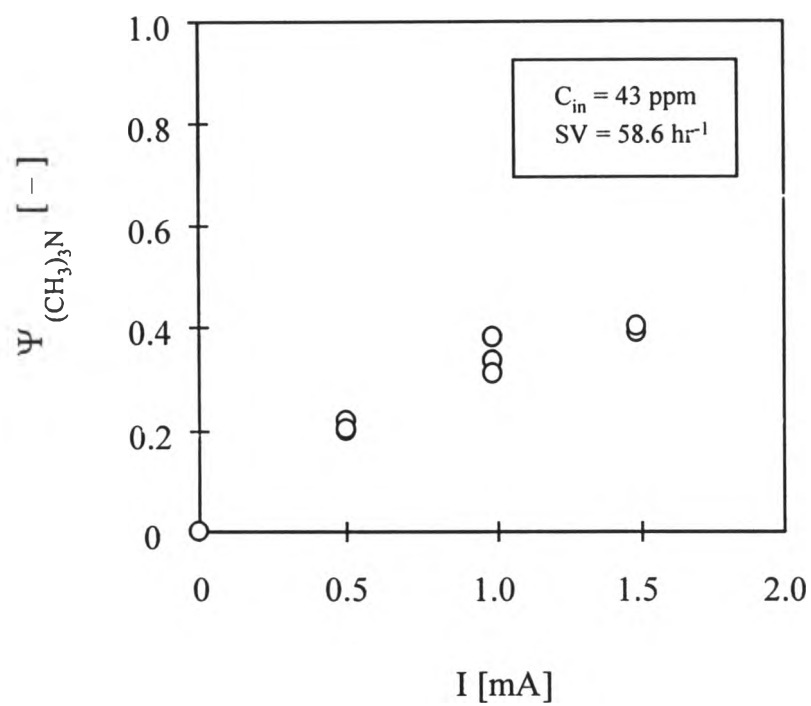
Figure 4.3   Removal efficiency of trimethylamine [(CH$_3$)$_3$N]
           from N$_2$

The reaction by-product is methane [CH_4], which was identified using GCMS at 1.5 mA discharge current and produced a peak area about 7% of the inlet concentration of $(CH_3)_3N$ in FID area (If the FID area of the inlet concentration of $(CH_3)_3N$ is 100, that of the reaction by-product appears about 7). **Figure 4.4** is the GCMS spectra on removal of $(CH_3)_3N$ from N_2. This figure shows the formation of CH_4 whose mass number is 16.

4.3.2.2 Removal of trimethylamine from N_2-O_2 mixture

In actual applications of gas purification, there are many cases of removals of gas impurities from air. Since air contains O_2 and a slight quantity of H_2O, it is necessary to study the influence of O_2 and H_2O on the removal of gas impurities. **Figure 4.5** shows the experimental results. When the discharge current was increased even a little as 0.15 mA, $(CH_3)_3N$ disappeared below the FID detection level.

To explain such a high removal efficiency that an average of 11.34 gas molecules are removed by one electron, one might consider the role of ozonation reaction. When there was no coexisting O_2 in the gas mixture, no O_3 was detected.

When O_2 coexists with trimethylamine [$(CH_3)_3N$], the removal mechanism becomes more complicated than when trimethylamine is removed from N_2 because electrons may attach to O_2 to produce O_3. In the experiment to remove $(CH_3)_3N$ from N_2-O_2 mixed gas, reaction by-products are generated. It is important to identify the reaction by-products generated in the corona discharge reactor. In this work, by-products are identified by GCMS. The inlet concentration of $(CH_3)_3N$ is 86 ppm, total flow rate is 91 cc/min and 20% of O_2 at 1.5 mA discharge current. The lists of by-products generated have been shown in **Table 4.5**.
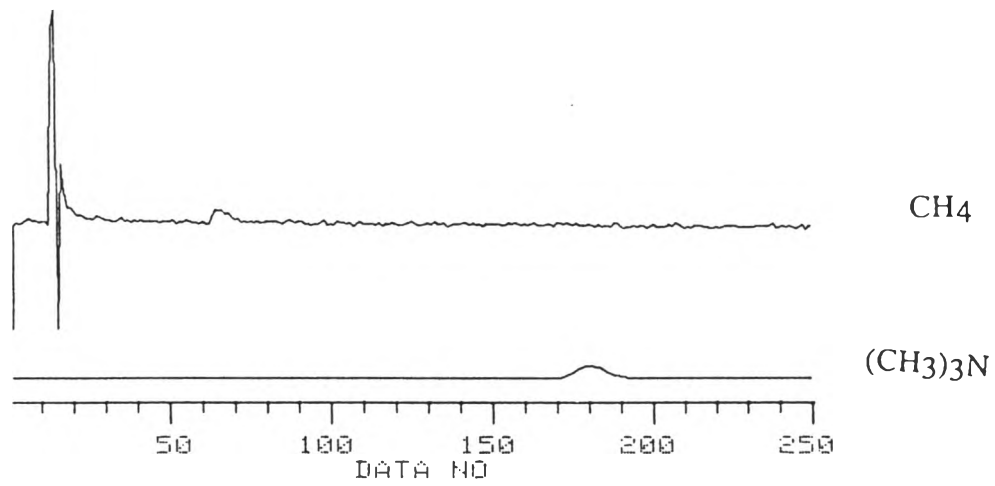
(a) Analysis of inlet gas by GCMS
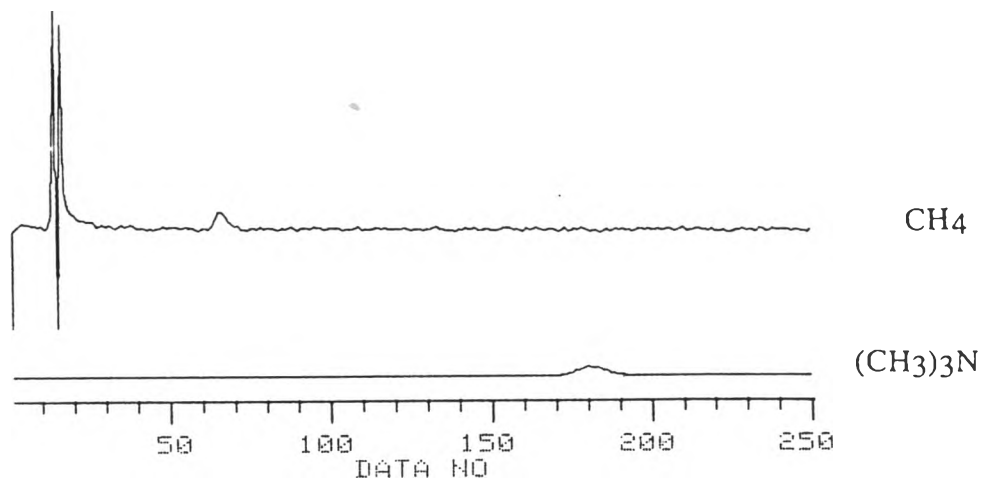
(b) Analysis of outlet gas by GCMS

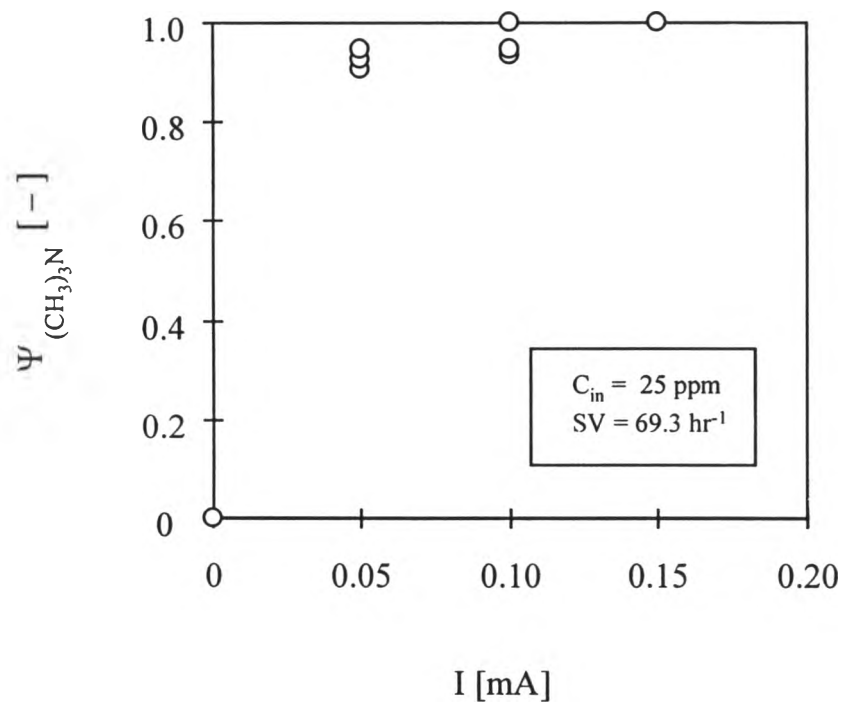Figure 4.4   GCMS spectra on removal of $(CH_3)_3N$ from N_2

Figure 4.5 The removal efficiency of trimethylamine [(CH$_3$)$_3$N]

from N$_2$-O$_2$ mixed gas; C$_{O2}$ = 20%

One can see that reaction by-products increase with the discharge current. **Figure 4.6** shows the GCMS spectra on the removal of $(CH_3)_3N$ from N_2-O_2 mixed gas.

Table 4.5 List of by-products generated on the removal of $(CH_3)_3N$ from N_2-O_2 mixed gas

No.	Retention Time(sec)	M/Z	M/Z of fragment	By-product	Amount at 0.05 mA	Amount at 0.1 mA
1	1.7	44	43, 42, 29, 28, 27	CH_3CHO	2%	5%
2	3.3	46	45, 44, 30, 31, 29	C_2H_5OH	4%	4%
3	4.9	58	57, 42, 29, 28, 27	$(CH_3)_2CO$	-	3%
4	6.9	61	60, 46, 45, 30, 29	CH_3NO_2	17%	19%[*]

* The amount of by-product 19% means that if FID area of inlet concentration of $(CH_3)_3N$ is 100, that of by-products generated is about 19.

- It is postulated that $(CH_3)_3N$ reacts with O_3 to become C_2H_5OH and CH_3NO_2, then C_2H_5OH undergo partial oxidation by O_3 to form CH_3CHO (Eq. 4.9). Acetone is a derivative from isopropyl alcohol $((CH_3)_2CHOH)$ which could be obtained by substituting 1 hydrogen atom of C_2H_5OH by 1 methyl group (Waddams, 1980, p. 162).

- The postulated reactions of by-products are reasonable because part of C_2H_5OH by-product is further changed to CH_3CHO and $(CH_3)_2CO$, so their total sum is more or less equal to that of CH_3NO_2.

4.3.2.3 Influence of H_2O on removal of trimethylamine from N_2

Figure 4.7 shows the removal efficiency of $(CH_3)_3N$ from N2 as a function of the discharge current, I, at different concentrations of H_2O, C_{H2O}. As for the influence of H_2O, the presence of H_2O significantly raises the removal efficiency, Ψ.
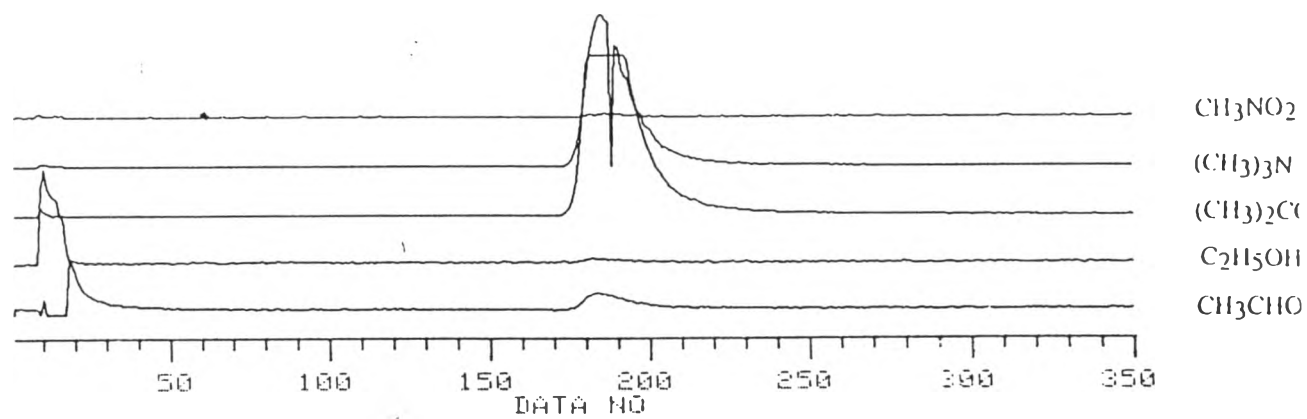
(a) Analysis of inlet gas by GCMS
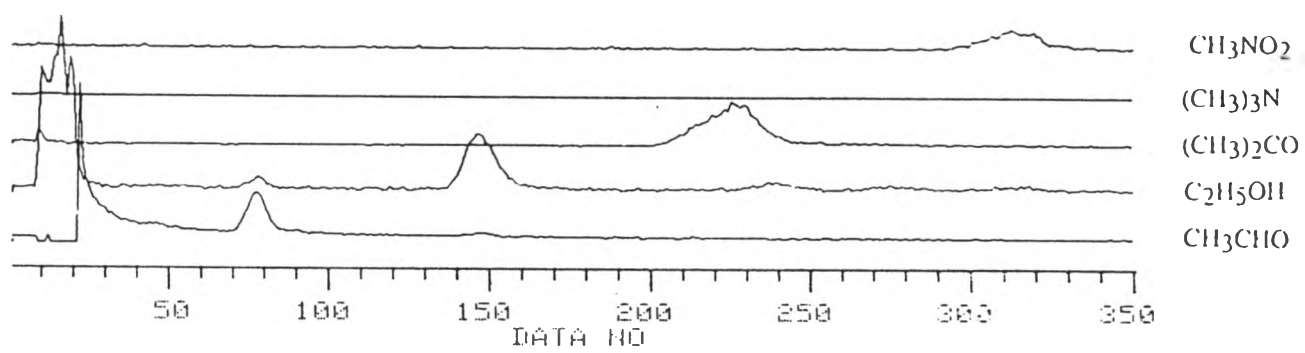
(b) Analysis of outlet gas by GCMS

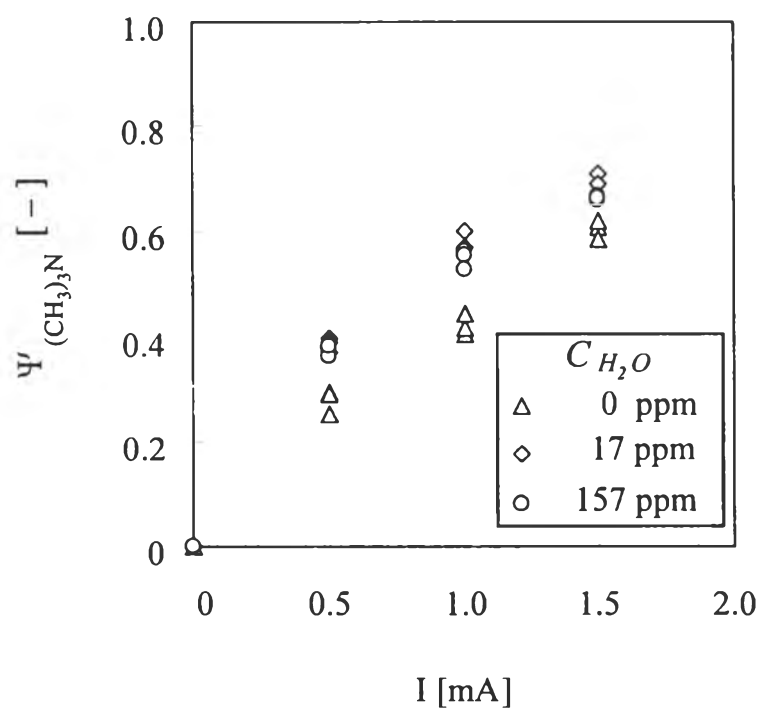Figure 4.6 GCMS spectra on removal of $(CH_3)_3N$ from N_2-O_2

Figure 4.7   Influence of H_2O on removal of trimethylamine
from N_2, $C_{(CH3)3N}$ = 81 ppm, SV = 75.9 hr^{-1}

In summary, the removal efficiencies of $(CH_3)_3N$ from N_2 in the presence of O_2 or H_2O become higher compared with those without coexisting O_2 or H_2O. Therefore, it may be concluded that the proposed gas purification method is applicable for removal of trimethylamine from N_2 and air.

4.3.2.4 Influence of SO_2 on removal of trimethylamine from N_2-O_2

Some experiments to observe the influence of SO_2 on removal of $(CH_3)_3N$ from N_2-O_2 mixed gas (17% O_2) has been carried out. The inlet concentration of $(CH_3)_3N$ is 34 ppm. Total gas flow rate is 428 cc/min. As seen from **Figure 4.8**, when the discharge current is as low as 0.01 mA, the concentration of $(CH_3)_3N$ disappears at all three concentrations of SO_2. It should be noted that the outlet concentration of $(CH_3)_3N$ even in the absence of the discharge current is significantly lower than the inlet concentration of $(CH_3)_3N$, as shown in **Figure 4.9**. The absence can be attributed to the spontaneous reaction between $(CH_3)_3N$ and SO_2. Increasing the concentration of SO_2 clearly decreases the outlet concentration of $(CH_3)_3N$ at no discharge current. In addition, white particles are observed at the inner surface of the reactor. This is probably the product of the reaction between $(CH_3)_3N$ and SO_2. **Figure 4.10** shows the effect of the discharge current on the change of SO_2 concentration, which is detected by Derivative Spectrophotometer, in the experiments to observe the influence of SO_2 on the removal of $(CH_3)_3N$ from N_2-O_2 mixed gas. One can see that the concentration of SO_2 decreases with the discharge current. However, it is difficult to effectively remove SO_2 with a low discharge current.

Two reaction by-products are observed in the outlet gas mixture in the experiment to investigate the influence of SO_2 on the removal of $(CH_3)_3N$ from N_2-O_2 mixed gas. The peak area of each reaction by-product is approximately 3% of that of the inlet concentration of $(CH_3)_3N$ at 0.03 mA with 192 ppm of coexisting SO_2. One reaction by- product is the same as by-product No.1 and the
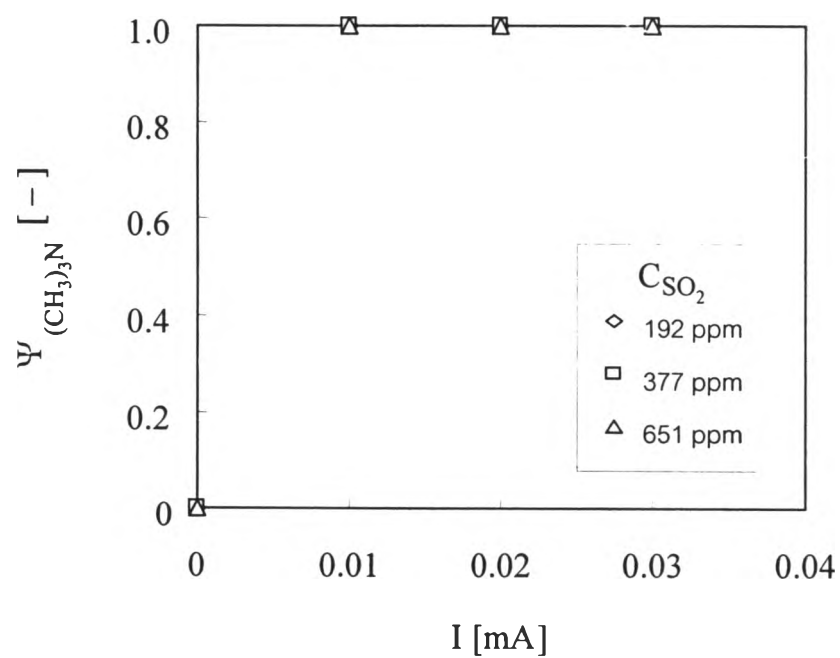
Figure 4.8   Influence of SO_2 on removal of $(CH_3)_3N$ from N_2-O_2;

$C_{(CH3)3N}$ = 34 ppm, C_{O2} = 17 % and SV = 80.9 hr^{-1}
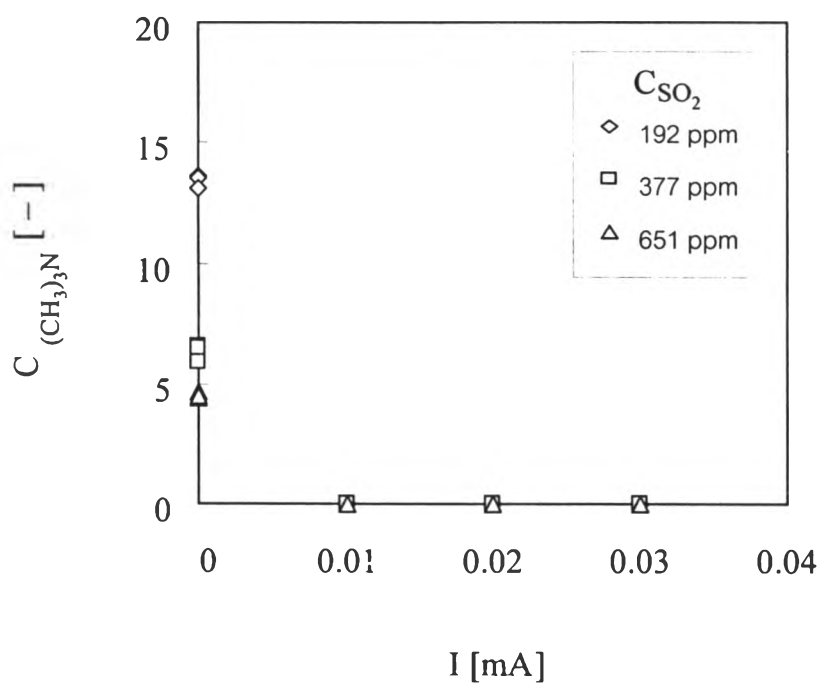
Figure 4.9   Decrement of $(CH_3)_3N$ on removal of SO_2 and $(CH_3)_3N$
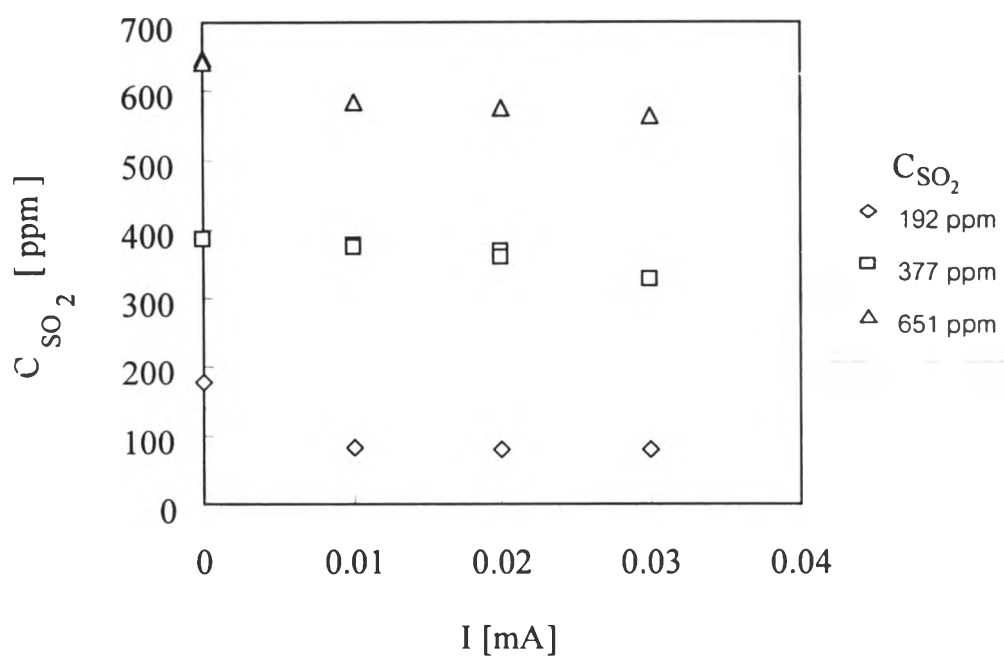
from N_2-O_2; $C_{(CH3)3N}$ = 34 ppm, C_{O2} = 17 % and

SV = 80.9 hr^{-1}

Figure 4.10   Concentration of SO_2 on removal of $(CH_3)_3N$ from N_2-O_2

other is by-product No.3 in **Table 4.5** because of the same retention time in FID detection.

4.3.2.5 Influence of SO_2 on removal of trimethylamine from N_2

Here experiment has been carried out to confirm the postulated reaction between $(CH_3)_3N$ and SO_2. The results are given in **Figure 4.11**. The inlet concentration of $(CH_3)_3N$ is 34 ppm and total flow rate is 426 cc/min. The outlet concentration of SO_2 against the discharge current is plotted in **Figure 4.13**. It can be seen from **Figure 4.11** that when electrons are provided, $(CH_3)_3N$ is removed even if O_2 does not coexist. But the removal efficiency of $(CH_3)_3N$ without coexisting O_2 is lower than the case of coexisting O_2 due to the absence of ozone effect. Even at zero discharge current, the outlet concentration of $(CH_3)_3N$ is significantly lower than the inlet concentration of $(CH_3)_3N$, as shown in **Figure 4.12**. The decrease can be attributed to the reaction between $(CH_3)_3N$ and SO_2. The reaction mechanism can be represented by **Equations 4.2** and **4.3**. The reaction among sulfur dioxide, trace oxygen and trace water to produce sulfuric acid could have occurred (Duecker and West, 1959).

The overall reaction is $\quad 2SO_2 + O_2 + 2H_2O \longrightarrow 2H_2SO_4 \quad \Delta H_{25} = -54.6\,\text{kcal} \quad (4.2)$

Type of reaction	Reaction
Homogeneous	$2NO + O_2 \longrightarrow 2NO_2$
Heterogeneous	$SO_2 + H_2O \longrightarrow H_2SO_3$
	$NO + NO_2 + H_2O \longrightarrow 2HNO_2$
Heterogeneous	$NO + NO_2 + 2H_2SO_4 \longrightarrow 2ONOSO_2OH + H_2O$
Oxidation	$H_2SO_3 + 2HNO_2 \longrightarrow H_2SO_4 + 2NO + H_2O$
Hydrolysis	$ONOSO_2OH + H_2O \longrightarrow H_2SO_4 + HNO_2$

Massay (1976) has reported the associative detachment with rate constant at 300 K and energy release, as follows:

Reaction	Energy release (eV)	Rate constant $(x10^{-10}\,cm^3s^{-1})$
$O^- + 1/2N_2 \rightarrow NO + e$	5.1	2.2
$O^- + NO \rightarrow NO_2 + e$	1.6	5
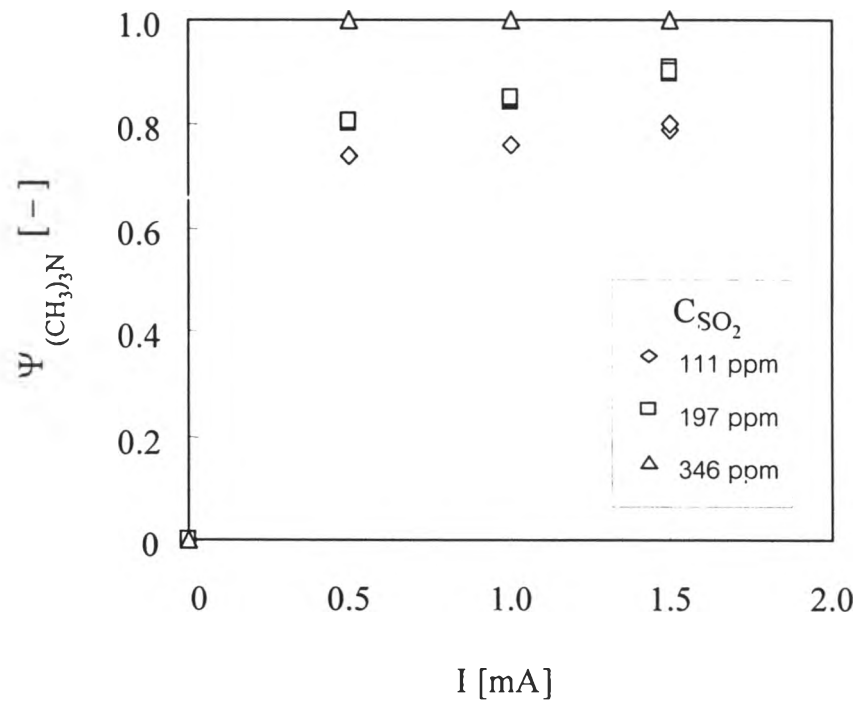
Figure 4.11   Influence of SO_2 on removal of $(CH_3)_3N$ from N_2; $C_{(CH3)3N} = 34$ ppm, SV = 80.5 hr^{-1}
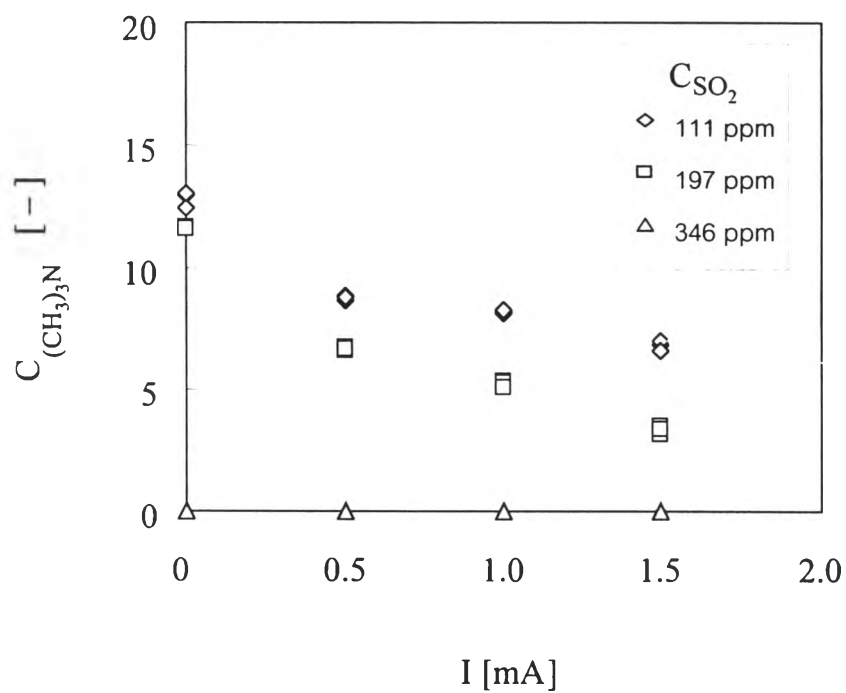
Figure 4.12   Decrement of $(CH_3)_3N$ on removal of SO_2 and $(CH_3)_3N$ from N_2; $C_{(CH3)3N}$ = 34 ppm, SV = 80.5 hr^{-1}
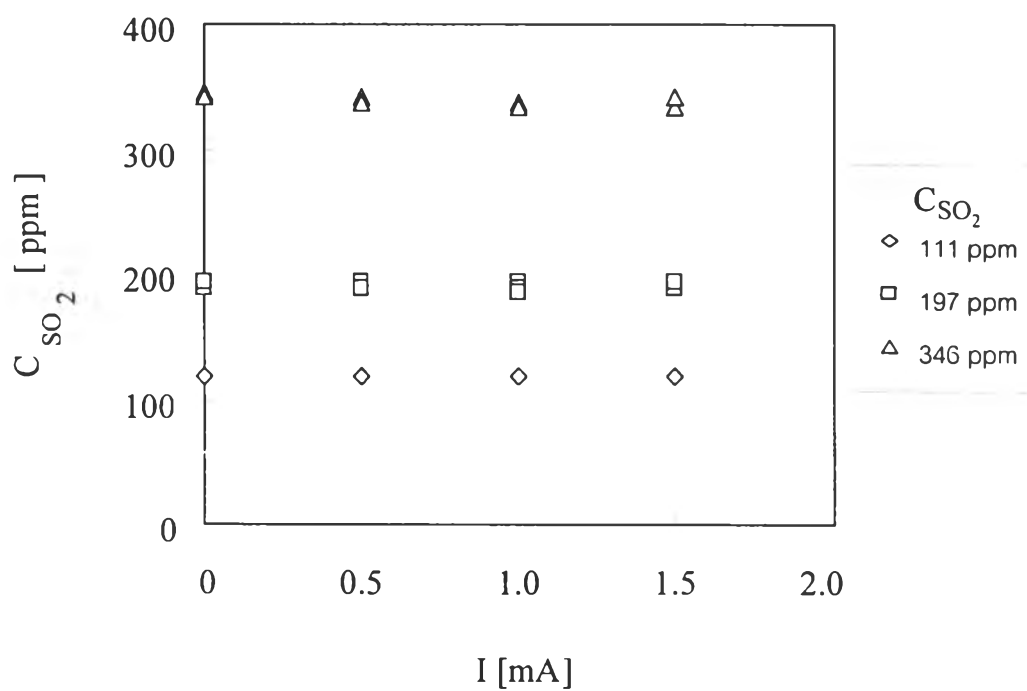
Figure 4.13   Outlet concentration of SO_2 on removal of $(CH_3)_3N$ from N_2;

$C_{(CH3)3N} = 34$ ppm, SV = 80.5 hr^{-1}

In section **4.3.3.5**, NO_2 previously removed and accumulated on the anode surface could serve as the catalytic oxides of nitrogen to produce H_2SO_4. Subsequently H_2SO_4 reacts with trimethylamine to form trimethyl ammonium hydrogen sulfate, $(CH_3)_3NHHSO_4$ or trimethyl ammonium hydrogen bisulfate, $[(CH_3)_3NH]_2SO_4$ which should be a solid salt at ambient temperature like ammonium sulphate salt.

Postulated Reaction Mechanism

$$(CH_3)_3N \; + \; H_2SO_4 \longrightarrow (CH_3)_3NHHSO_4 \quad (4.3a)$$

$$(CH_3)_3N \; + \; H_2SO_4 \longrightarrow [(CH_3)_3NH]_2SO_4 \quad (4.3b)$$

concluded that SO_2 exerts a catalytic effect on the electron attachment reaction of $(CH_3)_3N$ in the absence of O_2. Judging from the results in **Sections 4.3.2.4** and **4.3.2.5** it can be concluded that the presence of O_2 is essential to the simultaneous removal of SO_2 and $(CH_3)_3N$. It may be surmised that SO_2 is oxidized to SO_3 by O_3 in the presence of O_2. The reaction from SO_2 to SO_3 is an exothermic reversible reaction as indicated in **Equation 4.4** (Shreve, 1956).

$$2SO_2 \; + \; O_2 \longleftrightarrow 2SO_3 \quad (4.4)$$

As another way to explain the increase in the removal efficiency with coexisting O_2, we might consider the formation of ion-clusters with sulfur compound molecules. Lakdawala and Moruzzi (1981) have reported the experimental observations of clusters induced by negative ions of O_2 with several SO_2 molecules. **Equations (4.5)** and **(4.6)** has been proposed to describe these cluster formations.

$$O_2^- + n\,SO_2 \longrightarrow O_2^-(SO_2)_n \quad (n = 1,2,\ldots) \quad (4.5)$$

$$O^- + n\,SO_2 \longrightarrow O^-(SO_2)_n \quad (n = 1,2,\ldots) \quad (4.6)$$

4.3.3 Removal of acetaldehyde

This section is concerned with the removal of a prevalent malodorous gas, namely, acetaldehyde (CH_3CHO). Acetaldehyde can readily be produced in high temperature circumstances, such as during waste incineration.

4.3.3.1 Removal of CH_3CHO from N_2

Figure 4.14 shows the removal results of CH_3CHO from N_2. Here the removal efficiency of CH_3CHO, η_{CH3CHO}, as defined by **Equation 4.1** is plotted against the discharge current, I. These results indicate that the deposition-type reactor is applicable to the removal of CH_3CHO from N_2 even when the concentration of CH_3CHO is extremely low.

It has been reported that dissociative electron attachment of CH_3CHO may produce O^-, C_2O^-, HC_2O^-, CH_3CO^- or CH_3^- (Dressler and Allan, 1985). The selectivity to produce these ions depends on the level of electron energy. However, rate constant of the dissociative electron attachment of CH_3CHO has not been reported.

The amount of reaction by-product detected by the FID gas chromatograph is negligible. When electrons attach to CH_3CHO and negative ions are formed by electron attachment, they drift to the anode and are removed at the anode surface by deposition.

4.3.3.2 Removal of CH_3CHO from N_2-O_2 mixture

Figure 4.15 shows the influence of coexisting O_2 on the removal efficiency of CH_3CHO. To determine the influence of the concentration of the coexisting O_2, C_{O2} has been varied up to 20%. In these removal experiments,
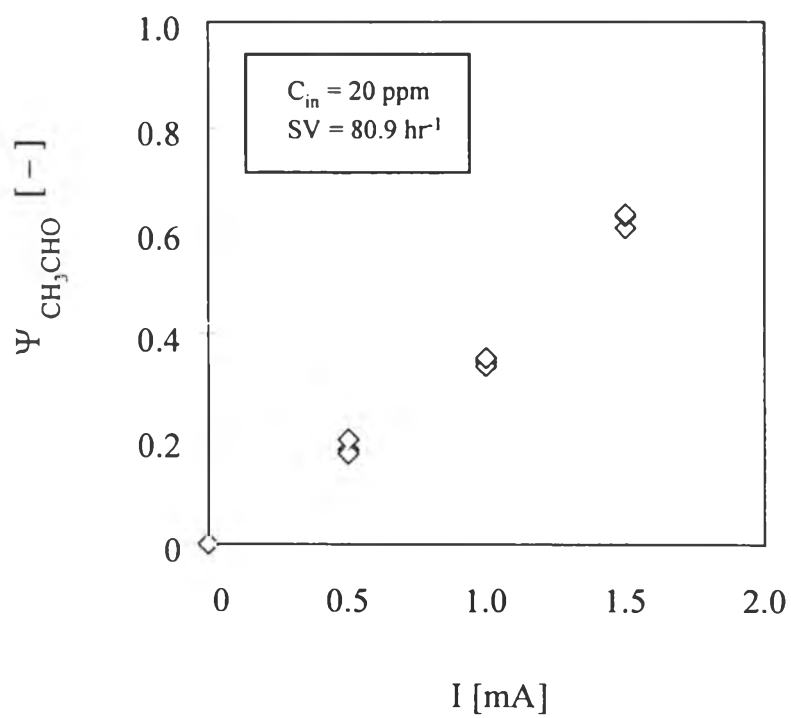
Figure 4.14   Removal of CH₃CHO from N₂
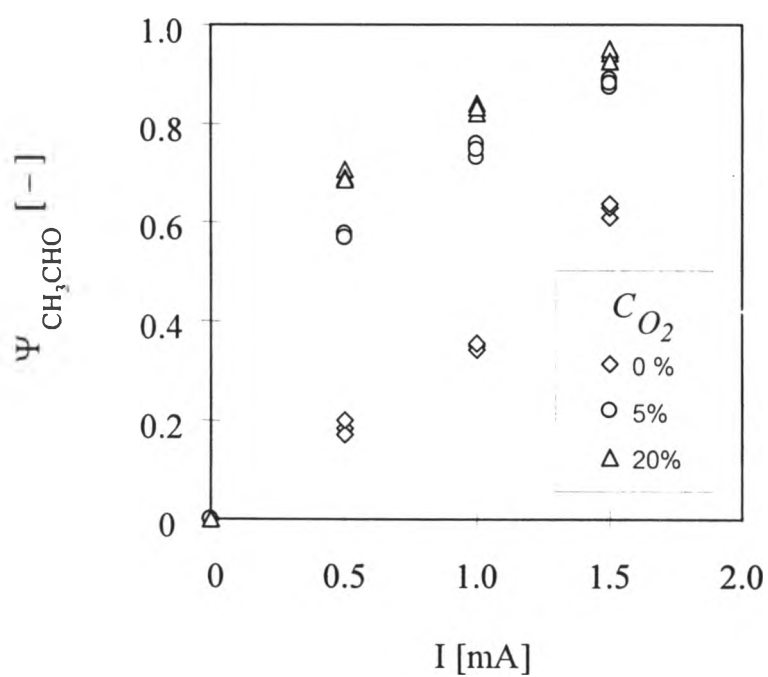
Figure 4.15   Removal of CH₃CHO fromN₂ in presence of O₂:

$C_{CH3CHO} = 20$ ppm, SV= 80.9 hr⁻¹

the formation of reaction by-products is negligible. This figure shows that the presence of O_2 enhances Ψ_{CH3CHO}. In **Section 4.4**, it has been shown that ozone (O_3) is produced by corona discharge in the air. Sano (1997) has reported that the reaction of CH_3CHO with O_3 improves the removal efficiency. Compared with the removal result by the corona-discharge reactor in the presence of O_2, one can see that almost a half of the removal efficiency can be attributed to the reaction with O_3.

It is also possible to think that clusters of O^- and CH_3CHO molecules are formed and they deposit at the anode. This cluster formation is written by **Equation (4.7)** (Sano, 1997)

$$O^- + mCH_3CHO^- \longrightarrow O^-[CH_3CHO]_m \qquad (4.7)$$

If the value of m in **Equation (4.7)** is large, the effect of the negative-ion cluster formation to improve the removal efficiency is large.

4.3.3.3 Influence of H_2O on removal of CH_3CHO from N_2

The influence of H_2O on the removal of CH_3CHO from N_2 was studied. **Figure 4.16** shows the removal efficiency of CH_3CHO, Ψ_{CH3CHO}, against the discharge current, I, at different concentrations of H_2O, C_{H2O}. As for the influence of H_2O, the presence of H_2O significantly raises the removal efficiency, Ψ.

Since the formation of reaction by-product was negligible, it may be concluded that CH_3CHO reacts with electrons to produce negative ions and the ions drift to anode surface to be removed by deposition.
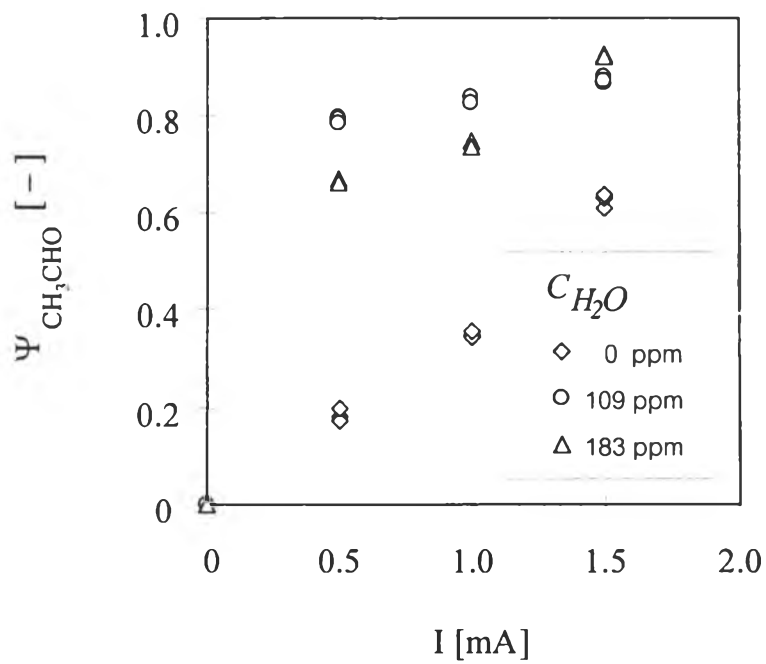
Figure 4.16 Removal of CH_3CHO from N_2 in presence of H_2O:

$C_{CH3CHO} = 20$ ppm, $SV = 80.9$ hr^{-1}

In conclusion, the removal efficiencies in the presence of O_2 or H_2O become higher compared with those without coexisting O_2 or H_2O. It means that the proposed gas purification method is applicable for removal of CH_3CHO from N_2 and dry air.

In the presence of H_2O, negative ions such as H^-, O^- and OH^- would be produced from the dissociative electron attachment of H_2O (Moruzzi and Phelps, 1966). The ions collect many CH_3CHO molecules to form clusters. The negative-ion clusters drift to the anode and deposit there.

4.3.3.4 Influence of gas flow rate on the removal efficiency of CH_3CHO from N_2

The influence of gas flow rate, Q, on the removal efficiency of $CH3CHO$, Ψ_{CH3CHO}, is given in **Figure 4.17** It can be seen that Ψ decreases as Q increases. This result is reasonable because an increase of Q causes a corresponding decrease in the residence time of the gas in this reactor.

4.3.3.5 Influence of NO_2 on removal of CH_3CHO from N_2-O_2

Influence of coexisting NO_2 on the removal of CH_3CHO from N_2-O_2 mixed gas has been investigated. NO_2 is mixed with 16 ppm CH_3CHO and 20% O_2 (balanced with N_2), and the total flow rate is 402 cc/min. Different concentrations of NO_2, which are analyzed with the Derivative Spectrophotometer, are mixed with CH_3CHO, N_2 and O_2. The relations between the removal efficiency of CH_3CHO and the discharge current at different NO_2 concentrations are shown in **Figures 4.18** and **4.20**.

When 482, 5492, 651 (**Figure 4.20**) and 668 (**Figure 4.18**) ppm of NO_2 is mixed with a CH_3CHO-N_2-O_2 mixed gas. The removal efficiency of CH_3CHO
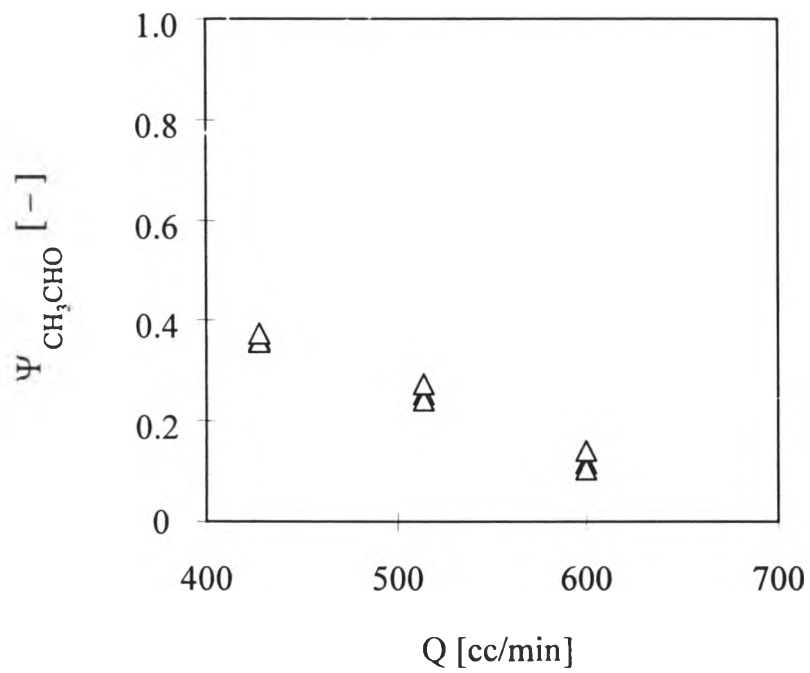
Figure 4.17   Influence of gas flow rate on removal of CH_3CHO from N_2:

C_{CH3CHO} = 20 ppm, I = 1 mA
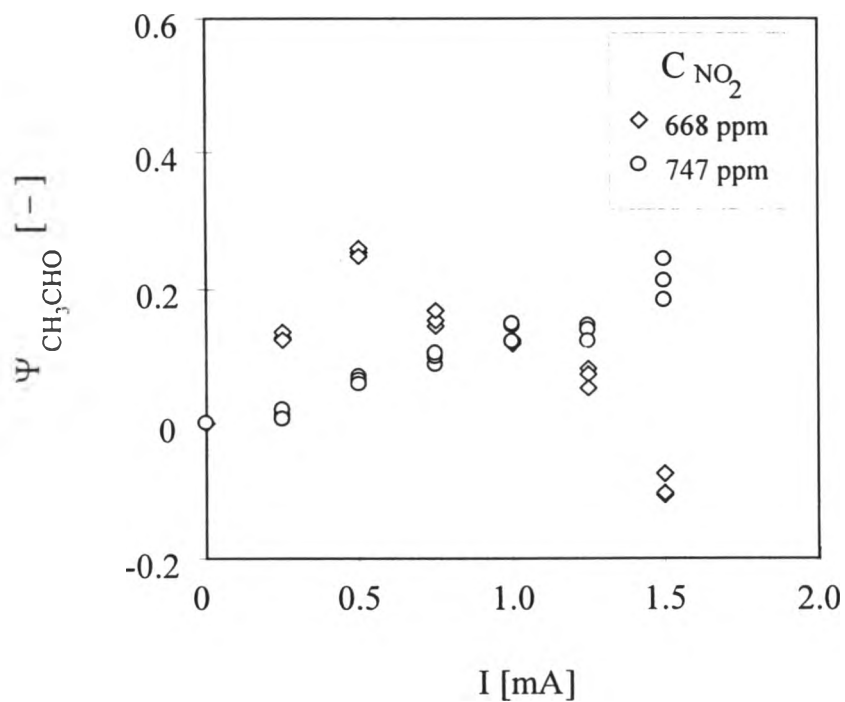
Figure 4.18 Removal of CH_3CHO from N_2-O_2 in presence of NO_2;
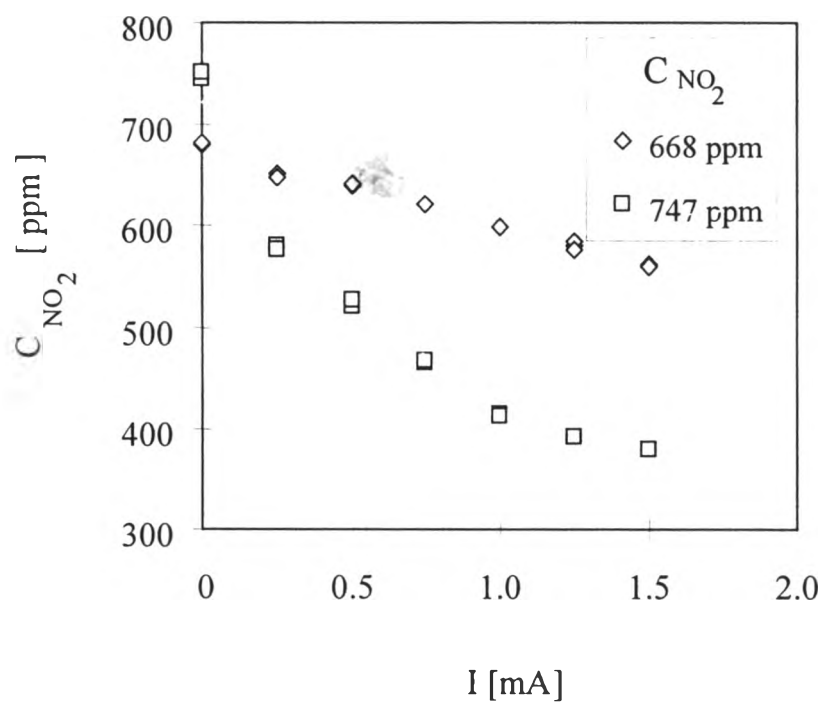
C_{CH3CHO} = 16 ppm, C_{O2} = 20% and SV = 76 hr-[1]

Figure 4.19 Decrement of concentration of NO_2 against discharge current during the removal of CH_3CHO from N_2-O_2
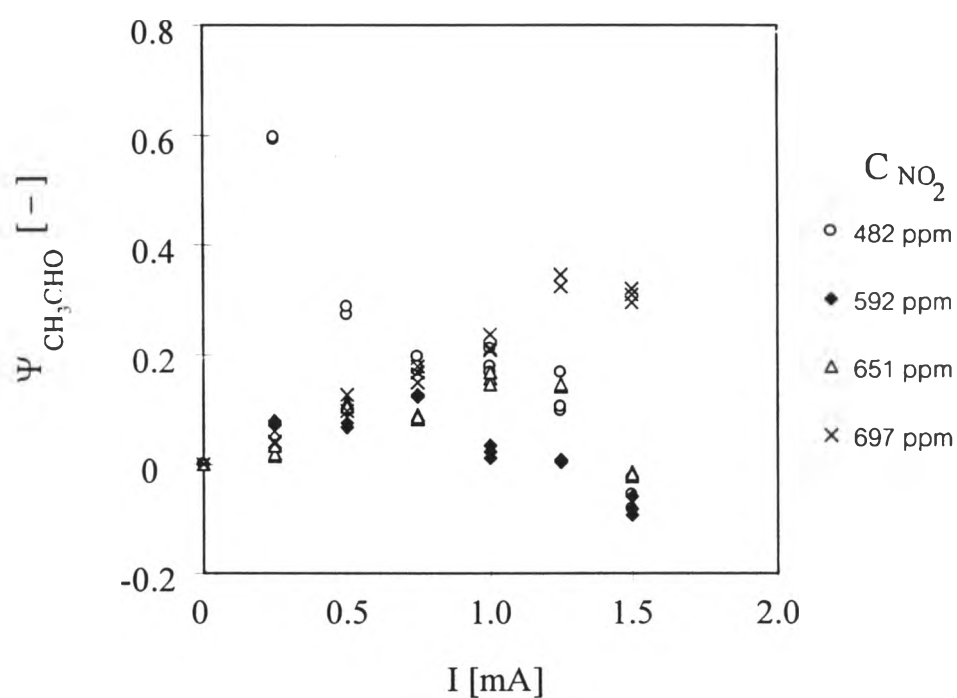
Figure 4.20 Removal of CH_3CHO from N_2-O_2 in presence of NO_2;

C_{CH3CHO} = 16 ppm, C_{O2} = 20% and SV = 75.8 hr-[1]

increases initially with the discharge current but subsequently decreases as the discharge current increases further. On the other hand, when 697 (**Figure 4.20**) and 747 (**Figure 4.18**) ppm of NO_2 is mixed with CH_3CHO-N_2-O_2 mixture, the removal efficiency consistently increases with the discharge current.

The results clearly indicate that a sufficiently high concentration (697 and 747 ppm) of coexisting NO_2 significantly promote the removal efficiency of CH_3CHO. Below 697 ppm NO_2 concentration, the beneficial effect on the removal of CH_3CHO is obtained only at low discharge currents. It is worth noting that the lower the NO_2 concentration, the lower the discharge current that still yields beneficial effect.

It is quite difficult to remove CH_3CHO from NO_2-O_2-N_2 mixture because on the average one electron can remove only 0.11 molecule of CH_3CHO at 1.5 mA discharge current. Above certain higher discharge current, the removal efficiency of CH_3CHO becomes minus because an apparent reaction by-product, which has the same retention time and mass number as CH_3CHO, is generated in this experiment. Several possibilities have been investigated. First, it is thought that the reactor wall is dirty after several experiments (with deposits of CH_3CHO) and desorption of CH_3CHO might have occurred when the discharge current is too high. After thorough cleaning and even after a brand-new reactor is used, the phenomenon of negative removal efficiency is still observed. Next the Teflon tubing system is changed to stainless steel but the phenomenon persists. It is noticed that the phenomenon disappears when O_2 does not coexist in the gas mixture.

It has already been proven in **Section 4.4** that ozone is produced when the gas mixture contains a sufficient concentration of O_2. If ethane exists as impurity in the feed gas, it can undergo successive partial oxidation by O_3 to become ethanol and acetaldehyde, as follows:

$$CH_3CH_3 \ + \ O_3 \ \longrightarrow \ CH_3CH_2OH \ + \ O_2 \qquad (4.8)$$

$$CH_3CH_2OH \ + \ O_3 \ \longrightarrow \ CH_3CHO \ + \ O_2 \ + \ H_2O \quad (4.9)$$

When the discharge current is relatively low, most electrons are used up in the removal of NO_2 and CH_3CHO and little O_3 is produced. When the discharge current is sufficiently large, there is an abundance if electrons and O_3 formation takes off. So ethanol or ethane impurity is turned into CH_3CHO, thus causing its removal efficiency to become negative.

However, when the inlet concentration of NO_2 is sufficiently high, more NO_2 is removed at 747 ppm than at 668 ppm inlet concentration of NO_2. So more electrons are used up and less remain to promote formation of O_3. That is why the strange phenomenon is not observed.

The decrement of the outlet concentration of NO_2 with the discharge current is depicted in **Figure 4.19**. In the case of 747 ppm coexisting NO_2, the outlet concentration of NO_2 is founded to be relatively lower than the case of 668 ppm coexisting NO_2. To have a better understanding on this phenomenon, some blank experiments on zero and different concentrations of NO_2 in N_2-O_2 (without CH_3CHO) are conducted. The objective is to measure the possible generation of NO_2 from N_2 and O_2 and the deposition of NO_2 in the absence of CH_3CHO.

Masuda and Nakao (1990) have reported that 80% of NO_2 is decomposed by corona discharges into N_2 and O_2. The reaction rates among electrons, NO_2 molecules and their decomposed species have recently been reviewed (Alekseev et al 1993), and various kinds of negative ion, such as NO_2^- (Herbst et al 1974), O_2^-, NO^- and O^- (Abouaf et al 1976) have been observed in NO_2 electron attachment experiments.

As shown in **Figure 4.21**, 0, 674 and 747 ppm of NO_2 is mixed with 20% O_2 balanced with N_2. The space velocity is 75.6 hr^{-1}. The results on the removal efficiency of NO_2 in **Figure 4.21** are quite similar to the results in **Figure 4.19**. When the inlet concentration of NO_2 is 0 ppm, there is no NO_2 generated from N_2 and O_2 in the reactor at all discharge currents. **Figure 4.21** explains why the removal efficiency of NO_2 at inlet NO_2 concentration of 747 ppm is comparatively higher than that at 668 ppm of inlet NO_2 in **Figure 4.19**.

4.3.3.6 Formation of CH_3CHO by-product with discharge current

To further investigate how CH_3CHO by-product could have been formed, a N_2-O_2 mixture is supplied to the reactor and discharge current is applied. **Figure 4.22** shows the outlet concentration of the observed by-product. The O_2 inlet concentration is 20%, and total flow rate is 401 cc/min. The concentration of the by-product increases with the discharge current and it has exactly the same retention time and mass number as CH_3CHO.

As mentioned earlier, the by-product may come from the detachment of previously deposited CH_3CHO inside the reactor or accumulated deposition of residual CH_3CHO in the gas line, from the decomposition of CH_3CHO precursor, or from chemical reaction of trace compounds in the inlet gas which leads to the formation of the by-product. When a clean or even new reactor is used, the by-product still does appear with the discharge current. Even after Teflon tube is substituted with SUS tube and glass is used instead of acrylic parts, the phenomenon still persists. Therefore, the reaction by-product can not come from detachment of previously deposited CH_3CHO inside the reactor, deposition of residual CH_3CHO in the gas flow line or the decomposition of CH_3CHO precursor.
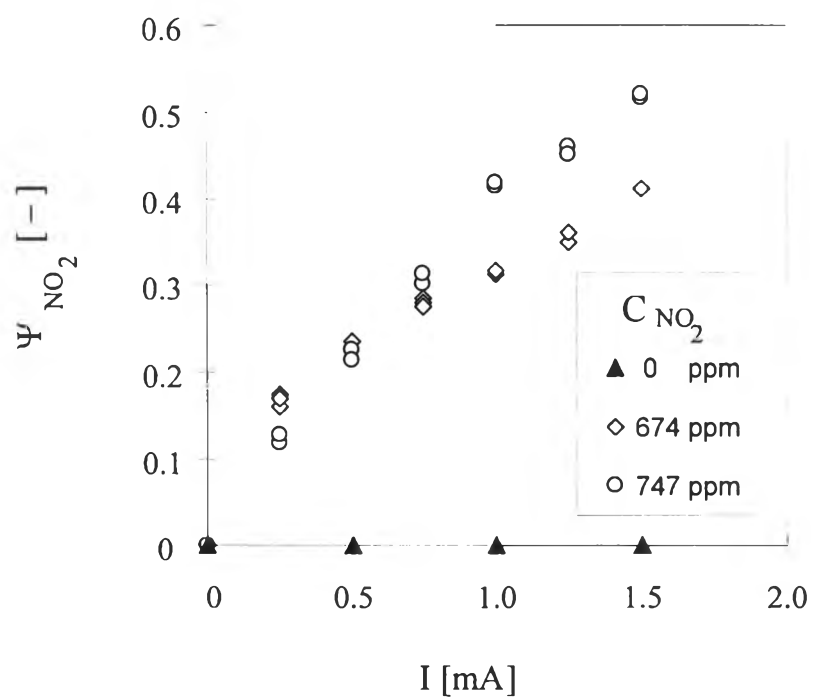
Figure 4.21 Removal of NO_2 from N_2-O_2; C_{O2} = 20%, SV = 75.6 hr^{-1}

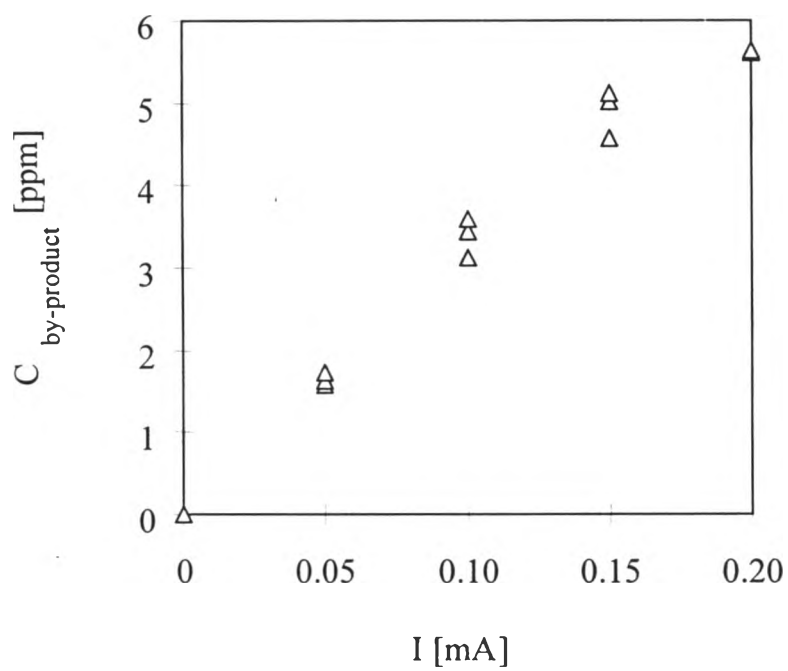Figure 4.22 Concentration of by-product generated from N_2-O_2 mixture; C_{O2} = 20%, SV = 75.8 hr^{-1}

It is very interesting that the by-product does not appear in the absence of O_2 and if another target gas, such as trimethylamine, is introduced in the N_2-O_2 mixture, the CH_3CHO by-product formation is suppressed. If water vapor and acetylene impurity exist, the possibility may be the chemical reaction of trace acetylene in the inlet gas. Acetaldehyde can be produced from acetylene by hydration. The initial product of the reaction is vinyl alcohol, which promptly rearranges itself to give acetaldehyde (Waddams, 1980), as seen in **Equation 4.10**.

$$HC \equiv CH + HOH \longrightarrow H_2C = CHOH \longrightarrow CH_3CHO \quad (4.10)$$
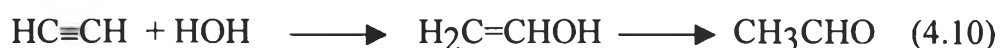
The formation of by-product (CH_3CHO) can explain why some removal efficiency in **Figure 4.18** becomes negative. Alternatively, the presence of ethane or ethanol impurity can explain not only the by-product formation but also why it is necessary to have O_2 in the mixture. Thus the latter explanation is more plausible.

4.3.3.7 Influence of SO_2 on removal of CH_3CHO from N_2-O_2

Experiments to investigate the influence of SO_2 on the removal of CH_3CHO from N_2-O_2 mixed gas have been carried out. SO_2 of two different concentrations is mixed with 16 ppm of CH_3CHO and 20% O_2 (balanced with N_2). The total flow rate is 402 cc/min.

As shown in **Figure 4.23**, the removal efficiency increases with the discharge current until 0.15 mA discharge current. After that the removal efficiency of CH_3CHO decreases with the discharge current. It is interesting that the presence of SO_2 retards the removal efficiency of CH_3CHO, even though in this experiment, the formation of reaction by-product is negligible. **Figure 4.24** shows the decrease of outlet concentration of SO_2 with the discharge current. It
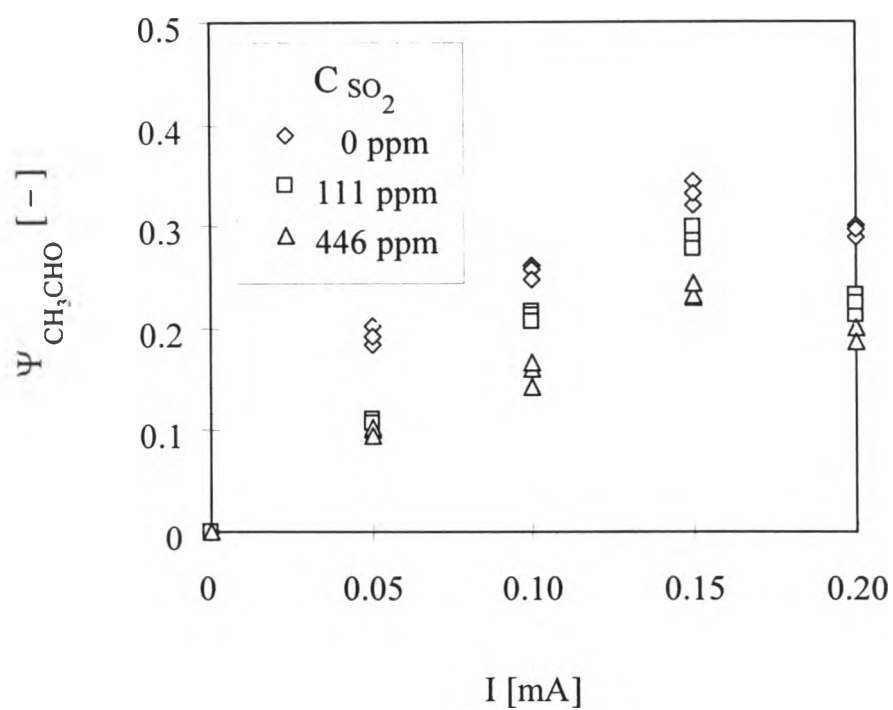
Figure 4.23 Removal of CH_3CHO in presence of SO_2 from N_2-O_2;

C_{CH3CHO} = 16 ppm, C_{O2} = 20% and SV = 76 hr-^{1}
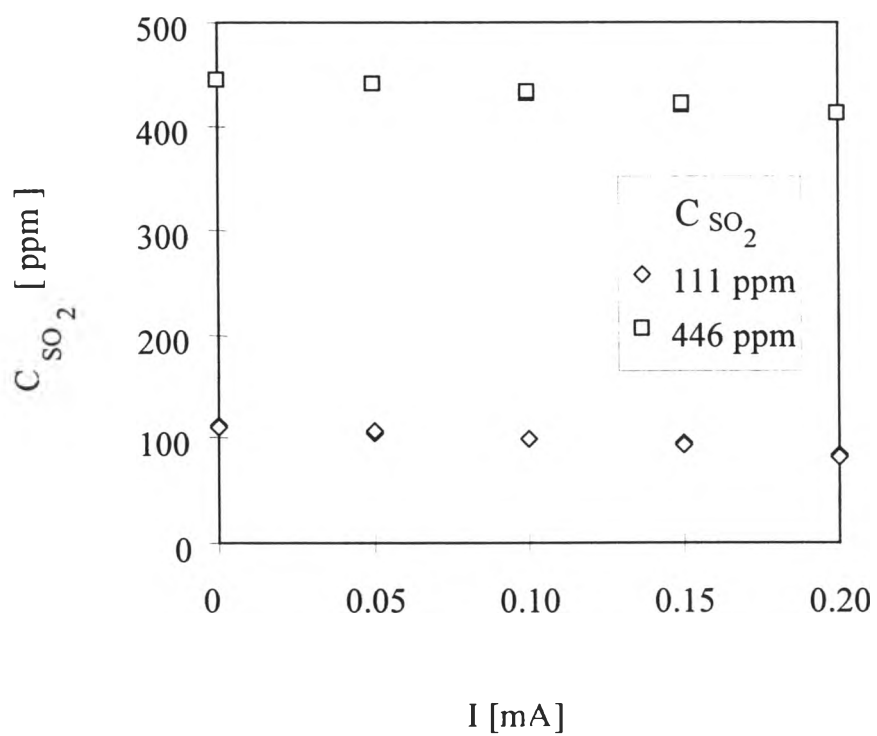
Figure 4.24 Decrement of concentration of SO_2 during CH_3CHO removal; from N_2-O_2 C_{CH3CHO} = 16 ppm, C_{O2} =20% and SV = 76 hr^{-1}

may be concluded that SO_2 is more highly electronegative and more abundant than CH_3CHO, so it takes up many electrons that should have attached to CH_3CHO.

4.3.3.8 Influence of CO_2 on removal of CH_3CHO from N_2-O_2

Figure 4.25 shows the influence of CO_2 on the removal of CH_3CHO from 20% O_2 (balanced with N_2). The retarding influence of coexisting CO_2 is not so significant at 0.05 and 0.1 mA discharge current. Above 0.15 mA discharge current, the retarding effect of CO_2 on CH_3CHO removal is obviously significant. The formation of reaction by-product is negligible in this experiment. It is postulated that CO_2 is less electronegative than CH_3CHO but the bonding strength of CO_2 molecules with the anode surface is stronger than that of CH_3CHO. Therefore, when a smaller number of electrons are available at low discharge currents, most electrons attach onto CH_3CHO and the deposit on the anode wall is composed of mostly CH_3CHO. At high discharge currents, there is an excess of electrons that can attach to CO_2. When the CO_2 ions deposit on the anode surface, they replace (drive off) some of the previously deposited CH_3CHO. Thus the CH_3CHO removal efficiency becomes lower at discharge currents above 0.15 mA.
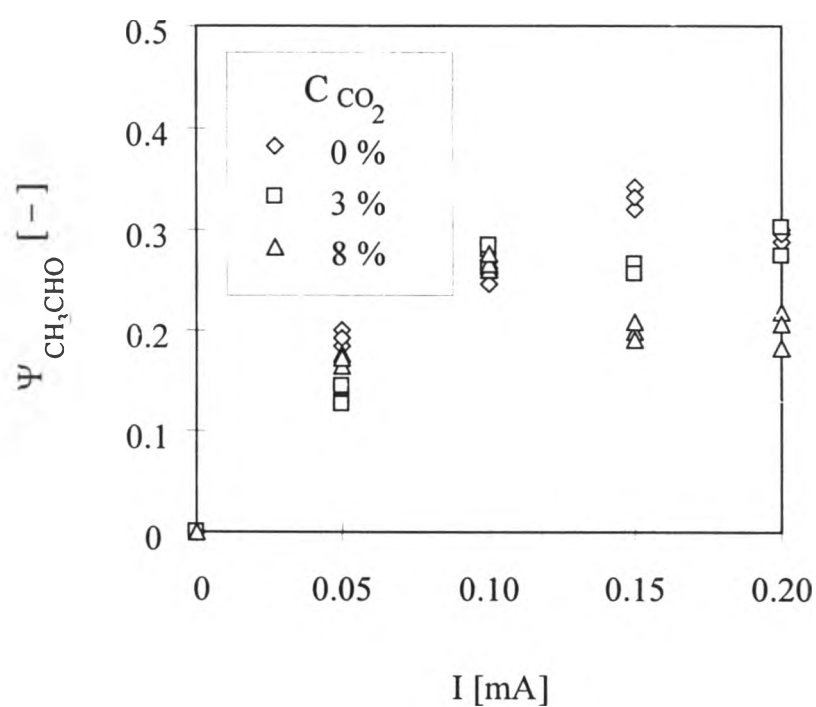
Figure 4.25 Removal of CH_3CHO in presence of CO_2 from N_2-O_2;

C_{CH3CHO} = 16 ppm, C_{O2} = 20% and SV = 75.3 hr-^{1}

4.3.4 Removal of ammonia

Noxious gases, such as ammonia, hydrogen sulfide and malodorous organic compounds are produced during biological decomposition and incineration of waste. These gases and odors can create health hazards for human and animals and create nuisance for neighboring communities.

4.3.4.1 Removal of NH_3 from N_2

Figure 4.26 (Data from Dr. Sano and Mr. Kittisak, 1996) shows the removal efficiency of NH_3 from inert gas (N_2-He mixed gas). Obviously, it is difficult to achieve a perfect removal. The inlet concentration of NH_3 is 49.2 ppm and the space velocity is relatively low at 188.5 hr^{-1}.

It is because NH_3 is weakly electronegative. Therefore, only a small portion of electrons manage to attach to NH_3 molecules, thus resulting in a low removal efficiency. At 1.5 mA discharge current, some of the deposited NH_3 may have detached from the anode surface.

4.3.4.2 Removal of NH_3 from N_2-O_2 mixed gas

An experiment to remove NH_3 from N_2-O_2 (20% O_2) mixture has been conducted. The concentration of NH_3 is measured by Spectrophotometer. **Figure 4.27** shows the removal efficiency against discharge current. When the discharge current is increased to 0.4 mA, NH_3 can no longer be detected with the Spectrophotometer. This experiment exhibits high removal efficiency as on the average 6.3 NH_3 molecules are removed by one electron.

Some reaction by-products are generated in the experiment to remove NH_3 from N_2-O_2.mixture. **Table 4.6** shows the list of probable by-products that

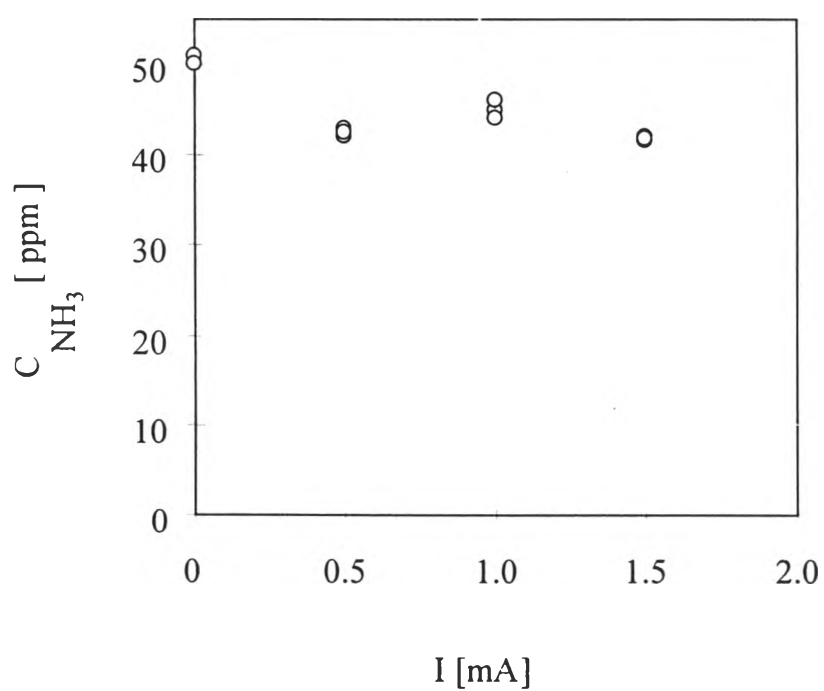Figure 4.26 Removal of NH_3 from inert gas (N_2-He mixed gas);

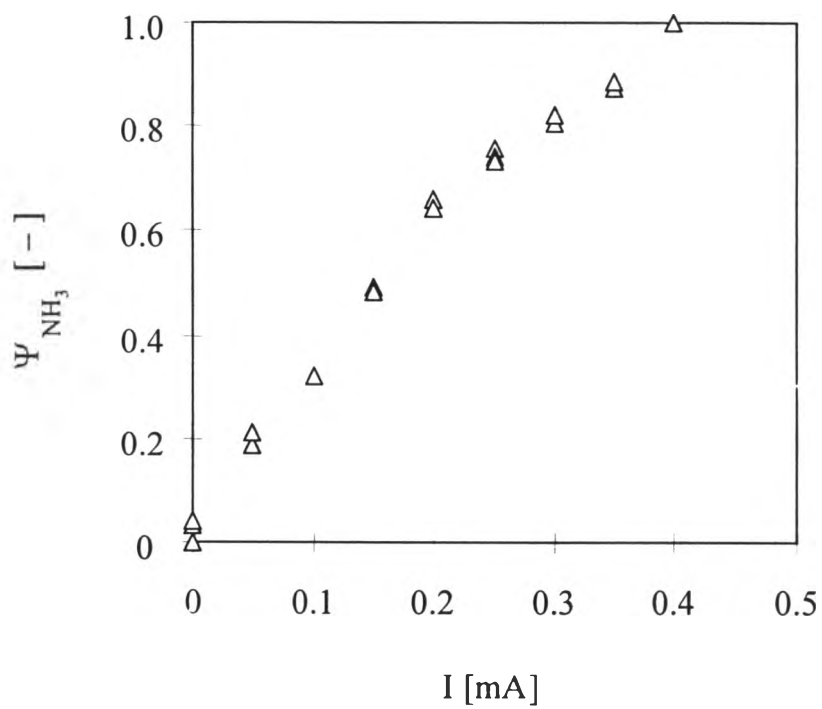$C_{NH3} = 49$ ppm, $SV = 188.5$ hr-[1] (Data from Dr.

Sano and Mr. Kittisak, 1996)

Figure 4.27 Removal of NH_3 from N_2-O_2 mixed gas);

$C_{NH3} = 96$ ppm, SV = 75.9 hr-[1]

can be interpreted from GCMS data. Since there are not enough detailed data, the reaction by-products can not successfully be identified yet. The ozone effect must have played a major role on NH_3 decomposition and removal.

Table 4.6 List of by-products on removal of NH_3 from N_2-O_2 mixture as interpreted from GCMS data

No.	Retention Time(sec)	M/Z	M/Z of fragment	Probable by-product	Change in by-product conc. with discharge current
1	1.8	44	43, 29, 15	H_2N_3	Increase
2	5.5	59	58, 43, 32, 28, 17, 16, 15, 14	HN_3O, N_4H_3	Increase

4.3.4.3 Influence of CO_2 on removal of NH_3 from N_2-O_2 mixture

To study the influence of CO_2 on the removal of NH_3 from N_2-O_2 mixed gas, 20% of O_2 and 141 ppm of NH_3 are mixed with 8% of CO_2. The total flow rate is 401 cc/min. **Figure 4.28** shows that the presence of 8% of CO_2 does not significantly affect the removal efficiency of NH_3 from N_2-O_2.

The reaction by-product has the same retention time in FID detection as reaction by-product no.1 in **Table 4.5**, that is, CH_3CHO.

4.3.4.4 Influence of H_2O on removal of NH_3 from N_2-O_2 mixture

Figure 4.29 shows the influence of H_2O on the removal of NH_3 from N_2-O_2. This figure shows the removal efficiency, Ψ_{NH3}, against the discharge current, I, at two different concentrations of H_2O, C_{H2O}. At discharge currents

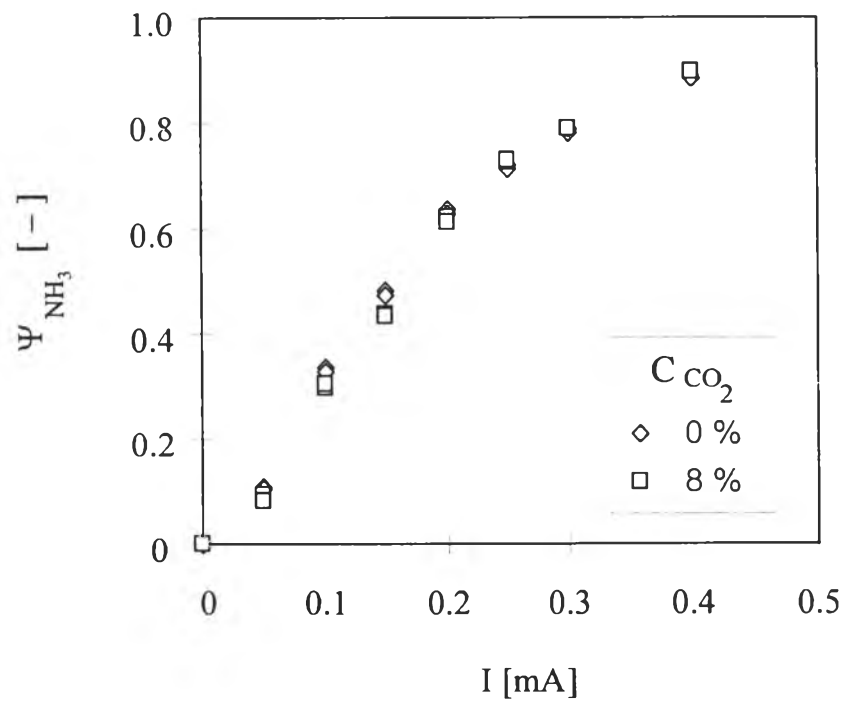Figure 4.28 Influence of CO_2 on removal of NH_3 from N_2-O_2;

C_{NH3} = 141 ppm, SV = 75.7 hr-^{1}
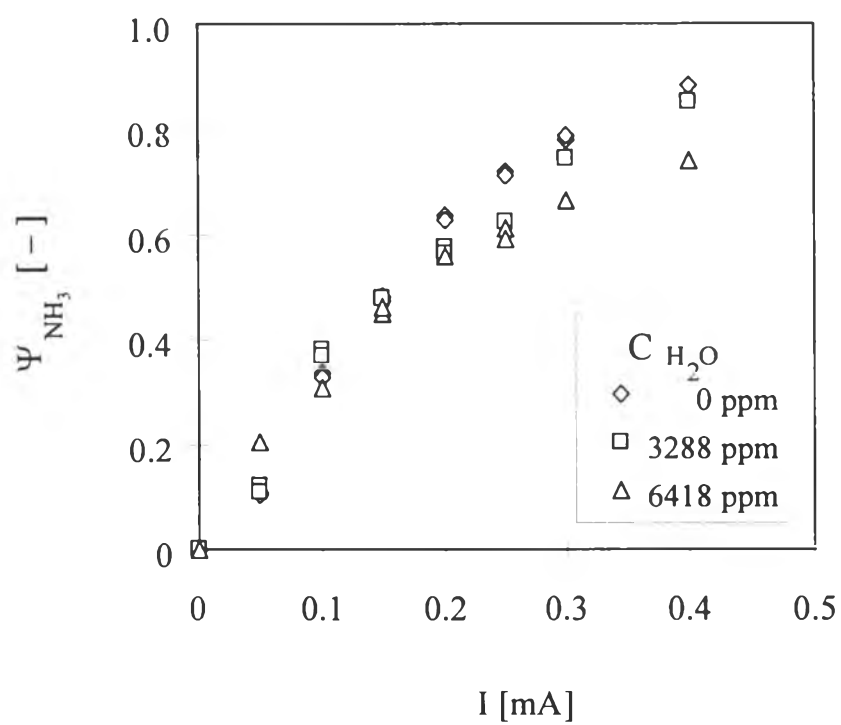
Figure 4.29 Influence of H_2O on removal of NH_3 from N_2-O_2;

$C_{NH3} = 143$ ppm, $SV = 75.6$ hr-[1]

above 0.2 mA, the retardation effect of H_2O on Ψ_{NH3} is obviously significant. At very low discharge current (0.05 mA), H_2O appears to have some beneficial effect on Ψ_{H2O}.

It is postulated that NH_3 is less electronegative than H_2O and O_2. At low discharge currents, only a small number of electrons are available to O_2 molecule to produce O_3, then NH_3 is removed via ozonation reaction. At high discharge currents, there is an excess of electrons that can attach to H_2O. They then interfere with the formation of ozone from oxygen. As the result, the NH_3 removal efficiency becomes lower at discharge currents above 0.2 mA.

4.3.4.5 Ammonia-sulfur dioxide reaction to form solid particles

To investigate the influence of SO_2 on the removal of NH_3 from N_2-O_2 mixture, SO_2 is mixed with NH_3 in N_2-O_2 mixture. What happens is that the concentration of SO_2 immediately decreases when the sample is measured with the Spectrophotometer at zero discharge current. This means that simultaneous reaction between NH_3 and SO_2 has occurred. In fact, different products of the anhydrous reaction between NH_3 and SO_2 have been reported in studies dating back to the nineteenth century (Divers and Ogawa, 1990; Scott et al., 1969). Basar-ur-Din and Aslan (1953) are the first to conclusively report that the products of the reaction are amidosulfurous acid (NH_3SO_2) and ammonium amidosulfite (($NH_3)_2SO_2$) at a temperature below 10°C in the absence of water vapor. Later Landreth et al (1974, 1985) repeat the equilibrium experiments on the formation of NH_3SO_2 and ($NH_3)_2SO_2$ and obtain equilibrium relations for temperatures in the range of 5°C to 45°C.

4.3.5 Simultaneous removal of trimethylamine and acetaldehyde from N_2-O_2

To study possible interaction between two reported crematory gas components, an experiment to remove $(CH_3)_3N$ and CH_3CHO from 20% O_2 (balanced with N_2) has been carried out. As seen from **Figure 4.30**, when the discharge current is as low as 0.05 mA, $(CH_3)_3N$ can not be detected with FID detector. The apparent removal efficiency of $(CH_3)_3N$ is high because one electron can remove 22.51 $(CH_3)_3N$ molecules at 0.05 mA discharge current . In contrast, one electron can remove only 0.23 molecule of CH_3CHO at 0.75 mA discharge current.

Some reaction by-products are generated on the removal of $(CH_3)_3N$ and CH_3CHO from N_2-O_2 mixed gas. The by-products in this experiment are similar to the reaction by-products observed in the removal of $(CH_3)_3N$ from N_2-O_2 mixed gas because they have the same retention times in FID detection. The concentrations of reaction by-products are found to increase with the discharge current.

As mentioned in **Section 4.4**, O_3 is produced when the gas mixture contains a sufficient concentration of O_2. The removal of trimethylamine can be attributed to the ozonation reaction. It is seen that the presence of CH_3CHO does not affect $(CH_3)_3N$ removal and the formation of CH_3CHO by-product disappears with coexisting $(CH_3)_3N$. It is thought that number of the electrons attach onto O_2, so there is less of electrons available to form CH_3CHO by-product.
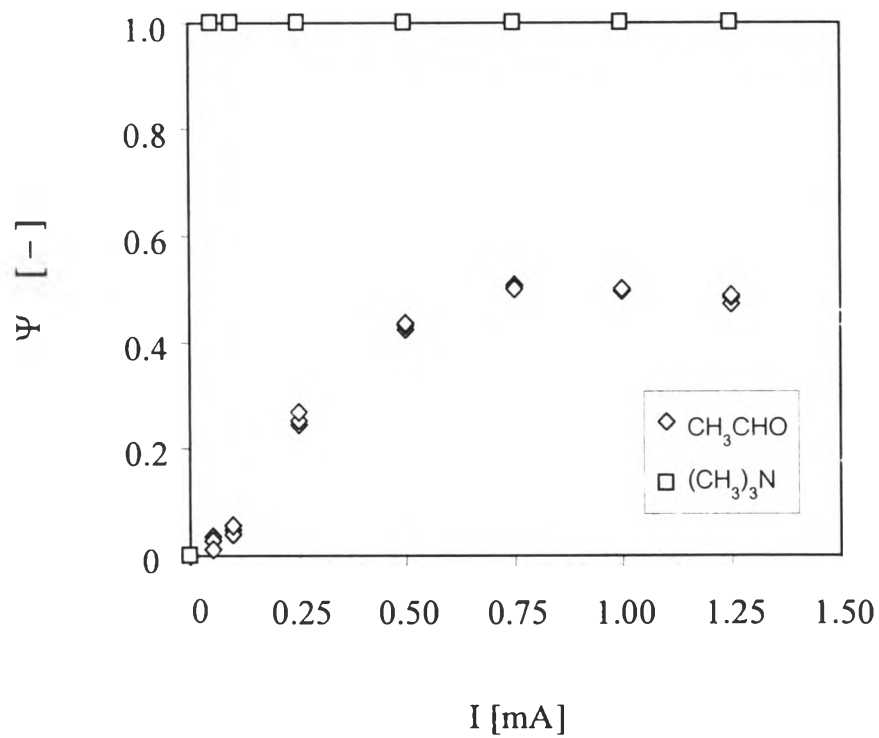
Figure 4.30   Simultaneous removal of CH_3CHO and $(CH_3)_3N$ from

N_2-O_2; $C_{(CH3)3N}$ = 43 ppm, C_{CH3CHO} = 15 ppm,

C_{O2} = 20%, SV = 75.0 hr-^{1}

4.3.6 Simultaneous removal of ammonia and acetaldehyde from N_2-O_2

An experiment has been carried out to observe the influence of NH_3 on the removal of CH_3CHO from N_2-O_2 mixed gas. NH_3 and CH_3CHO are mixed with 20% O_2 (balanced with N_2). As seen from **Figure 4.31**, when NH_3 coexists with CH_3CHO the removal efficiency of CH_3CHO from N_2-O_2 mixed gas is significantly enhanced. A maximum removal efficiency is achieved at 0.2 mA.

Figure 4.32 shows that in the copresence of CH_3CHO the removal efficiency of NH_3 is higher at 96 ppm than at 145 ppm of NH_3. It is because more electrons are available per NH_3 molecule, thus increasing their collision probability. Two reaction by-products are detected. They are similar to those produced from the removal of NH_3 from N_2-O_2 mixed gas.
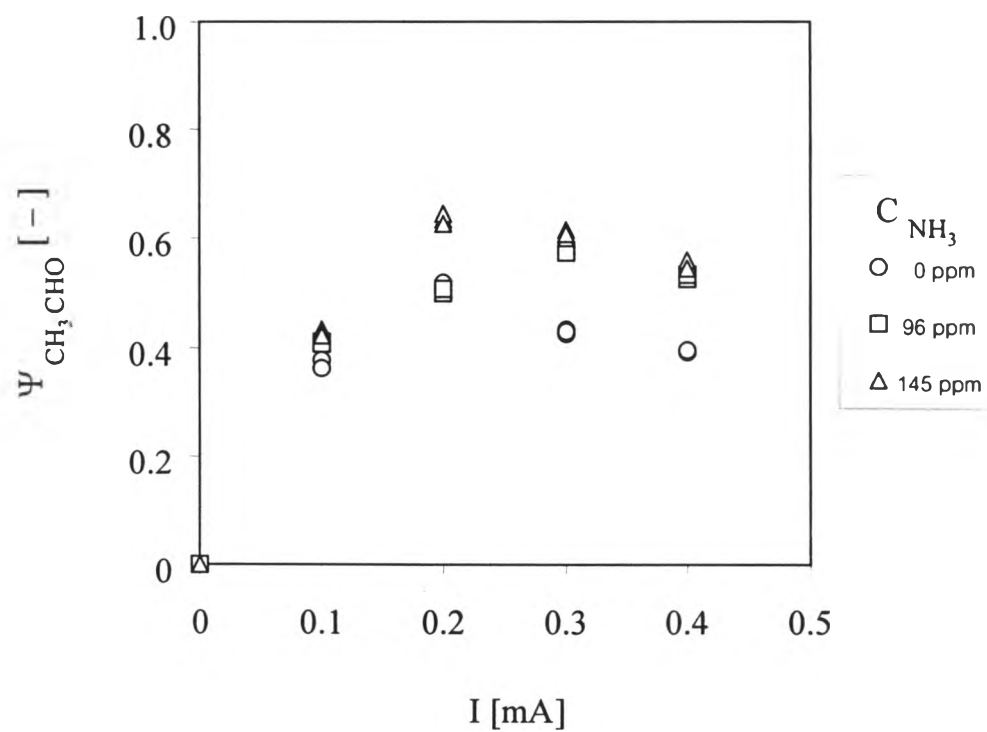
Figure 4.31   Removal of NH_3 and CH_3CHO from N_2-O_2;

C_{CH3CHO} = 16 ppm, C_{O2} = 20%, SV = 75.6 hr-1
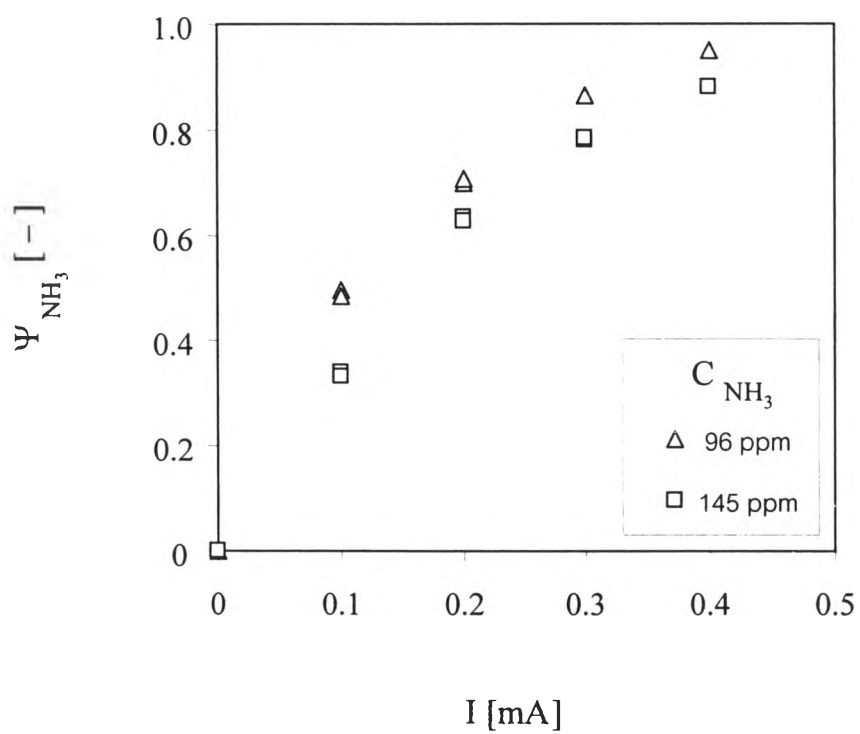
Figure 4.32 Removal of NH_3 on removal of NH_3 and CH_3CHO from

N_2-O_2; C_{CH3CHO} = 16 ppm, C_{O2} = 20%, SV = 75.6 hr-[1]

4.4 Substantiation of ozone effect

When O_2 is present in a gas mixture, it could react with electrons. Electron attachment on O_2 has been reported in the literature (Morruzzi and Phelps, 1966; Massay, 1976; Rapp and Briglia, 1976; Chantry and Schulz, 1967).

$$O_2 + e^- \longrightarrow O_2^- \tag{4.11}$$

$$O_2 + e^- \longrightarrow O + O^- \tag{4.12}$$
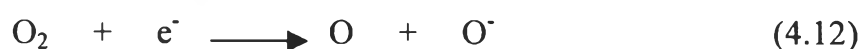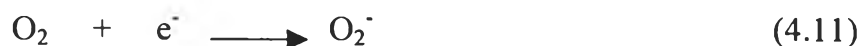
Moruzzi and Phelps (1966) report that the reaction in **Equation (4.11)** occurs in the low electron energy range ($E/p < 1.5$ $V.m^{-1}.Pa$). In contrast, the reaction of **Equation (4.12)** occurs in the higher electron energy range. Also in a corona-discharge reactor, the closer the electrons are to the cathode wire, the higher their energy level.

When O_2 collides with a high-energy electron near the cathode wire in the corona-discharge reactor, production of O^- is expected as in **Equation (4.12)**. Then O_3 is produced from reaction of O^- with O_2 (Loiseau et al., 1994; Hadj-Zaine et al., 1992).

In short, some ozone (O_3) is produced. Since O_3 is very reactive, the ozonation reaction is used in some commercial devices for deodorization and sterilization. The same ozonation reaction is expected to contribute to the removal of gas impurities in the present corona discharge reactor.

To substantiate the role of the ozonation reaction, two reactors are connected serially. **Figure 4.33** shows the apparatus to confirm the O_3 effect. N_2-O_2 mixture is supplied to the first reactor to produce O_3 by corona discharge. Then a gas impurity is mixed with the outlet gas from the first reactor, and the mixture is introduced to the second reactor. No voltage is applied on the second
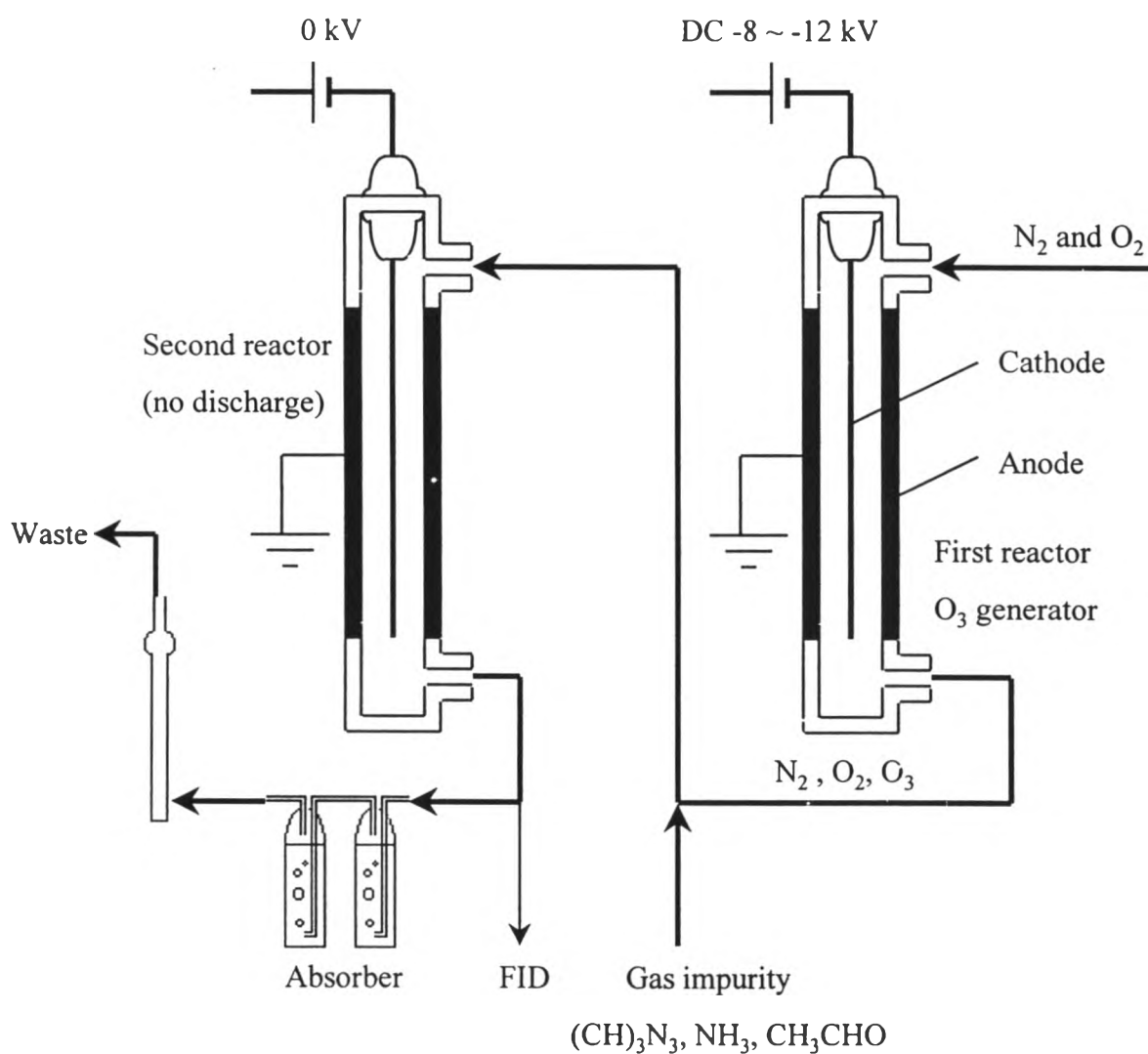
0 kV   DC -8 ~ -12 kV

N₂ and O₂

Second reactor
(no discharge)

Cathode

Anode

First reactor

O₃ generator

Waste

N₂ , O₂, O₃

Absorber   FID   Gas impurity

(CH)₃N₃, NH₃, CH₃CHO

Figure 4.33 Apparatus to substantiate O₃ effect

reactor, so there is no corona discharge in the second reactor, which only provides space for the reaction of ozone with the impurity. Then the change in the concentration of the impurity at the outlet of the second reactor is measured. The decrease in the outlet concentration from the second reactor gives the O_3 effect.

Figure 4.34 shows the formation of O_3 from N_2-O_2 mixed gas, 22% O_2. The concentration of O_3 at the first reactor outlet, C_{O3}, is plotted against the discharge current. By calculation, we estimate that one electron takes part in the production of 40 molecules of ozone at 0.05 mA. The change in the concentration of trimethylamine between the inlet and outlet of the second reactor is measured. The observed decrease in the impurity within the second reactor represents the O_3 effect as shown in **Figure 4.35**. Here it is found that 0.36 molecule of $(CH_3)_3N$ is removed by one molecule of O_3 at 0.05 mA discharge current. In this experiment, the detected reaction by-products are the same as those detected in the removal of $(CH_3)_3N$ from N_2-O_2 mixed, as shown in **Table 4.5**.
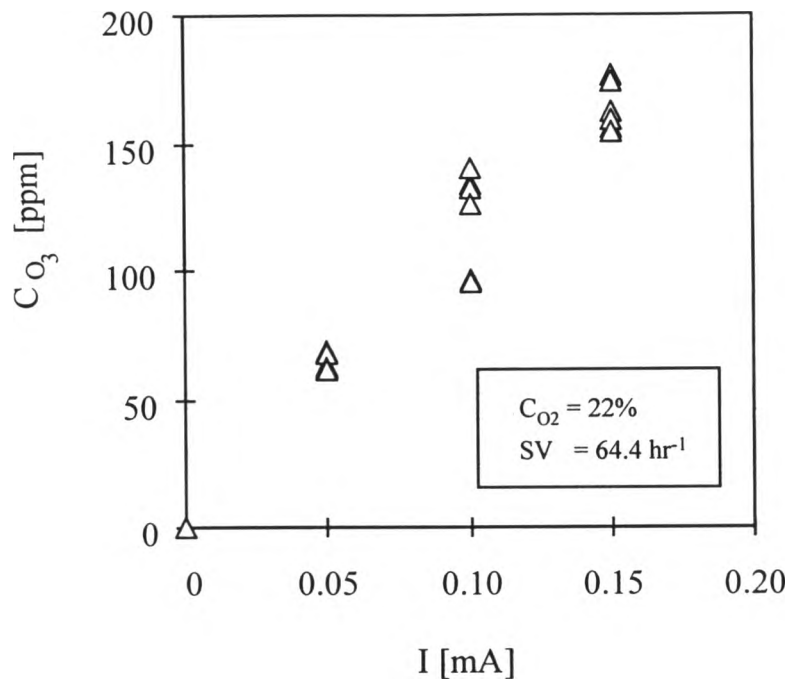
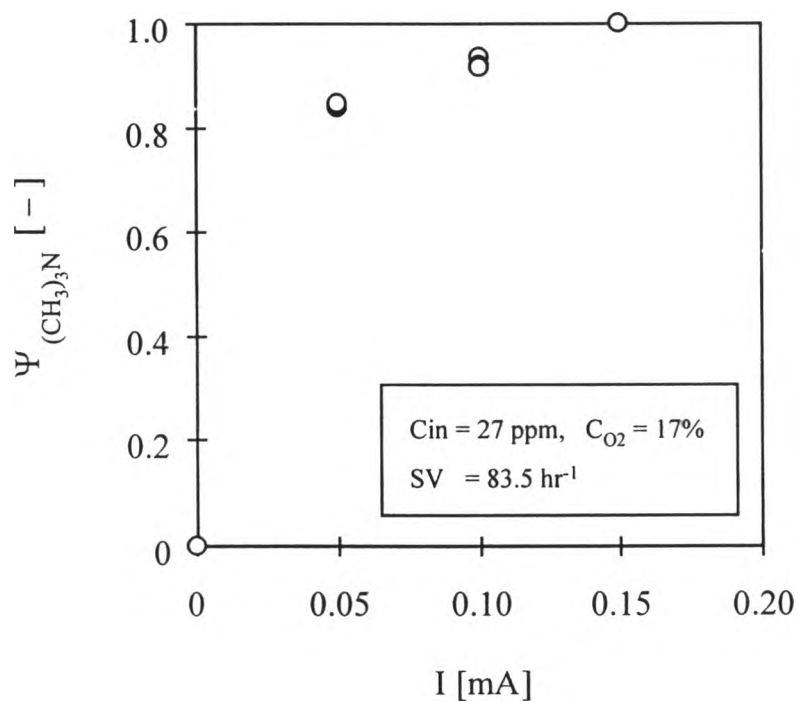Figure 4.34   Formation of O_3 from N_2-O_2 mixed gas in the first reactor

Figure 4.35   Effect of ozonation reaction on removal of trimethylamine

in the second reactor

4.5 Technique to reduce reaction by-products and improve removal efficiency

In the previous experiment to observe the influence of SO_2 on the removal of $(CH_3)_3N$ from N_2-O_2 mixed gas using single reactor, it is found that the concentration of $(CH_3)_3N$ disappears with the discharge current. Increasing the inlet concentration of SO_2 clearly decreases the outlet concentration of $(CH_3)_3N$ even at no discharge current. One can see that the concentration of SO_2 also decreases with discharge current. However, it is difficult to effectively remove SO_2 with a low discharge current and undesirable reaction by-products increase with the discharge current.

A two reactor system to reduce undesirable reaction by-products and to improve removal efficiency is proposed for the removal of $(CH_3)_3N$ and SO_2 from N_2-O_2 mixture. **Figure 4.36** shows a schematic diagram of the two-reactor system. The first reactor discharges low current mainly aims at the removal of $(CH_3)_3N$ while producing little reaction by-products. Then the second reactor discharges high current to effectively remove the remaining SO_2.

In the experiment, the concentrations of $(CH_3)_3N$, SO_2 and O_2 are 45 ppm, 81 ppm and 19% respectively. The total flow rate is 432 cc/min. Removal of $(CH_3)_3N$ at relatively low discharge currents is carried out in the first reactor and removal of the remaining SO_2 at higher discharge currents is carried out in the second reactor. The results are respectively shown in **Figures 4.37** and **4.38**.

In **Figure 4.37**, high removal efficiency of $(CH_3)_3N$ is achieved at a low discharge current because of the ozonation reaction. The reaction by-product generated in the first reactor is negligible. As for the removal of SO_2 in the second reactor **(Figure 4.38)**, high removal of SO_2 is achieved at 1.0 mA but some reaction by-products are detected, which have the same retention times as those found in the removal of $(CH_3)_3N$ from O_2-N_2 mixed gas. They might come
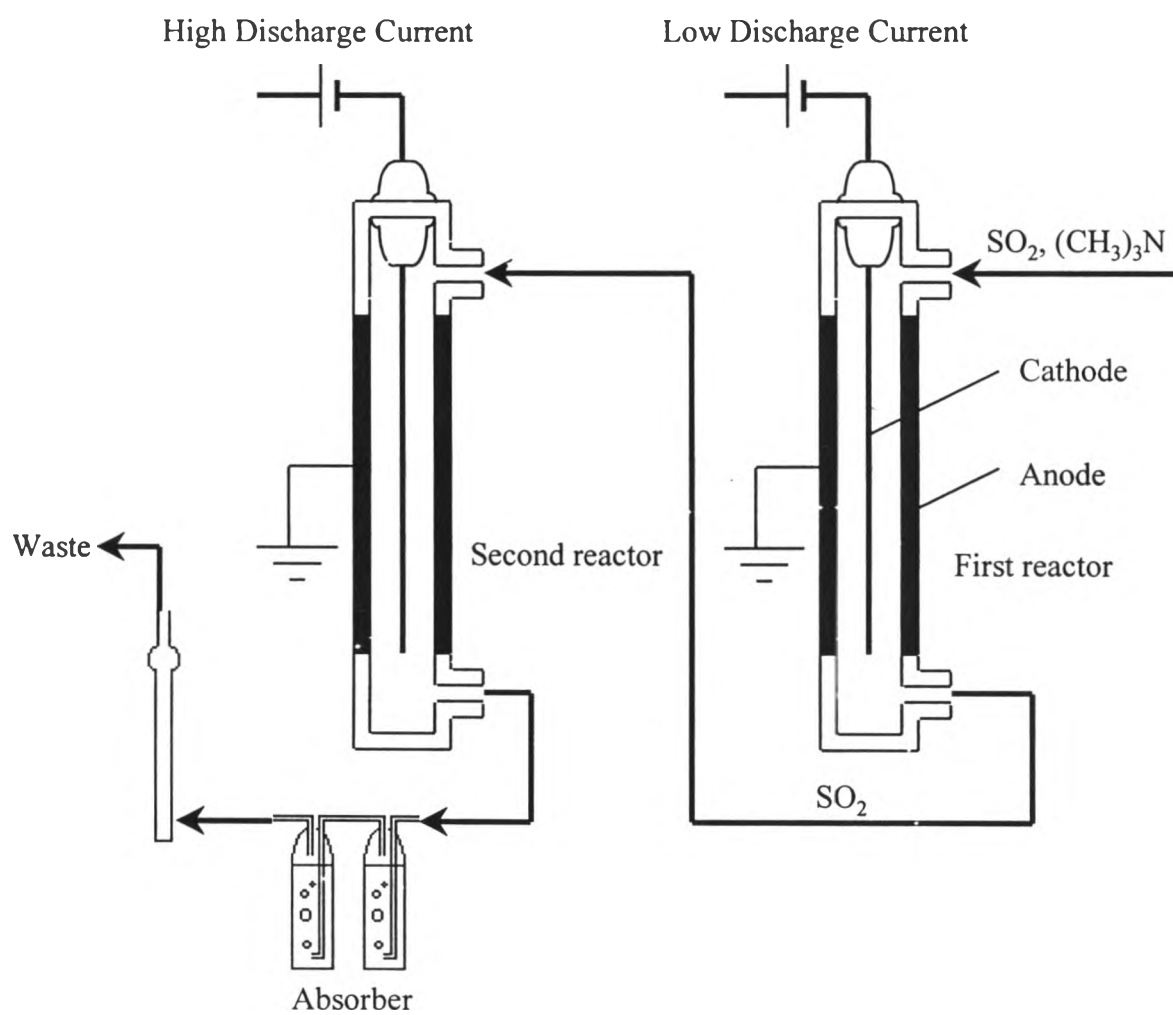
Figure 4.36 Removal of $(CH_3)_3N$ and SO_2 from N_2-O_2 using two reactor system
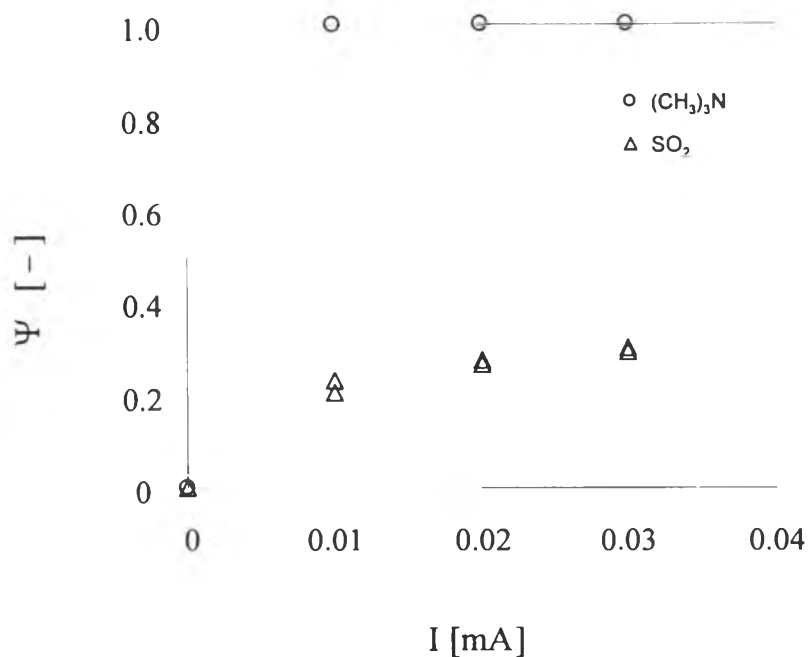
Figure 4.37   Removal of $(CH_3)_3N$ and SO_2 from N_2-O_2 in the first reactor;

$C_{O2} = 19\%$, $C_{(CH3)3N} = 45$ ppm, $C_{SO2} = 81$ ppm, $SV = 81.6$ hr-^{1}
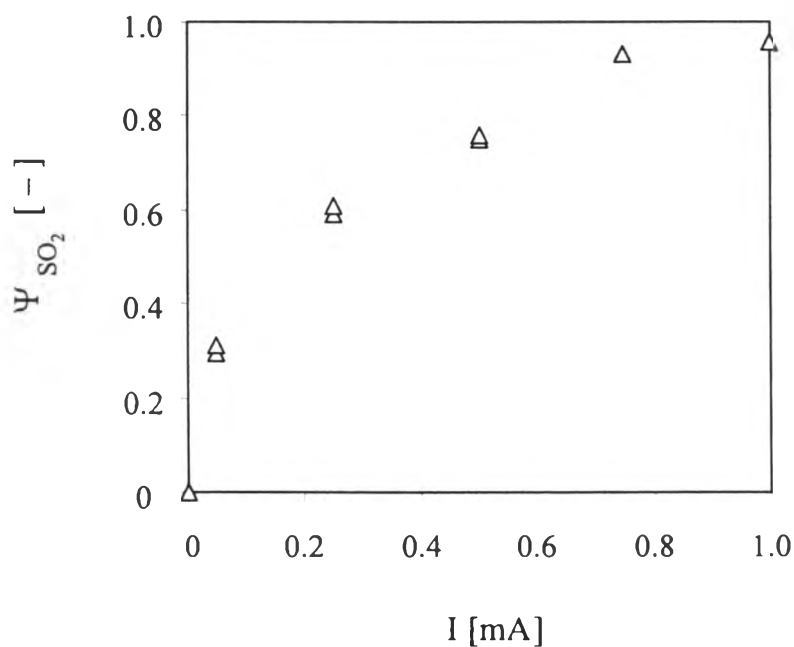
Figure 4.38 Removal of SO_2 in the second reactor; $C_{O2} = 19\%$

$C_{(CH3)3N} = 0$ ppm, $C_{SO2} = 81$ ppm, $SV = 81.6$ hr-^{1}

from the desorption of impurities at the anode wall of the reactor because the reactor has not been cleaned before use and very high discharge current (1.0mA) is applied.

By adopting a two-reactor system, it has been shown that essentially all $(CH_3)_3N$ can be removed in the first reactor and about 95% of SO_2 can be removed without any generation of undesirable by-products.